DOI: 10.1111/cgf.14333
EUROVIS 2021
N. Smit, K. Vrotsou, and B. Wang
(Guest Editors)

Volume 40 (2021), Number 3
STAR – State of The Art Report

Uncertainty-aware Visualization in Medical Imaging - A Survey

Christina Gillmann [1], Dorothee Saur[2], Thomas Wischgoll[3] and Gerik Scheuermann[1]

[1]Leipzig University, Germany
[2]Leipzig University, Medical Centre, Germany
[3]Wright State University, U.S.A

Abstract

Medical imaging (image acquisition, image transformation, and image visualization) is a standard tool for clinicians in order to make diagnoses, plan surgeries, or educate students. Each of these steps is affected by uncertainty, which can highly influence the decision-making process of clinicians. Visualization can help in understanding and communicating these uncertainties. In this manuscript, we aim to summarize the current state-of-the-art in uncertainty-aware visualization in medical imaging. Our report is based on the steps involved in medical imaging as well as its applications. Requirements are formulated to examine the considered approaches. In addition, this manuscript shows which approaches can be combined to form uncertainty-aware medical imaging pipelines. Based on our analysis, we are able to point to open problems in uncertainty-aware medical imaging.
Keywords: Medical Visualization, Uncertainty Visualization, Survey

1. Introduction

Medical imaging focuses on the analysis, visualization, and exploration of medical image data [PB14a]. It has an over 120 year old tradition [Bra08]. This journey started in 1895 with the discovery of the X-Ray which allowed clinicians to examine structures inside the human body without interfering with it. By now, medical imaging has developed into a standard tool to assist in various applications, such as diagnosis, determine treatment options, and show the health status of a patient, as shown in Figure 1. Here, medical doctors use medical imaging which separates into acquisition (green), transformation (red) and visualization (blue), for specific applications (yellow). Medical imaging has always been highly interconnected with visualization, as visualization holds the potential to make the captured medical images understandable and interpretable [PB07].

Medical imaging can be roughly separated into three different steps: Image Acquisition, Image Transformation, and Image Visualization. Depending on the purpose of the use of medical imaging, different image acquisition modalities can be considered. The available techniques include Ultrasound, Computed Tomography Scans, Magnetic Resonance Imaging, Diffusion Tensor Imaging, and Positron Tensor Imaging. All of these techniques produce unique data that are all affected by uncertainty due to different effects, such as the reconstruction process [Bru17] or patient motion [SP19]. In addition, each step in the medical imaging pipeline that transforms the input image can introduce additional uncertainty into the medical imaging process. This uncertainty highly influences the decision-making process of clinicians when dealing with medical image data [TWSM15]. This can lead to misinterpretation if not communicated properly [LWA*20] and can in the worst case have crucial consequences to the patients' health.

Hence, uncertainty information plays an important role [LWA*20] in medical imaging and the visualization process connected to it. The acquisition process, resulting images, and the needs of clinicians result in a special setup when considering uncertainty visualization. Uncertainty-aware visualization is a very active research field that has been addressed in a state-of-the-art analysis by multiple research groups. However, a state-of-the-art survey, which would highlight the special needs of uncertainty visualization has lastly been performed by Ristovski et al. [RPHL14] in 2014. Since then, there has been serious additional research efforts to enhance uncertainty-aware medical imaging, which are not recorded in a systematic way.

In this work, we aim to provide a starting point for medical visualization researchers to help find existing solutions in uncertainty-

Figure 1: *Medical imaging and its use. Clinicians can make use of different medical imaging techniques: In the acquisition step (green), images are generated that can be transformed throughout various technologies (red) and visualized (blue) with differing techniques. The selected medical imaging techniques can be applied to a variety of applications (yellow). The color-coding will be maintained to provide a smooth reading throughout the manuscript.*

aware visualization of medical imaging. Our primary goal is to provide an easy to understand classification scheme that suits the understanding of visualization researchers in the context of medical imaging. In addition, we aim to identify open problems in uncertainty-aware medical imaging.

Therefore, this manuscript contributes:

- A taxonomy of sources of uncertainty in medical imaging
- A state-of-the-art analysis of uncertainty-aware visualization in medical imaging
- A workflow chart directly indicating potential workflows in uncertainty-aware medical imaging
- A list of open problems in uncertainty-aware visualization in medical imaging

STAR Scope State-of-the-art Reports (STARs) related to uncertainty visualization have been conducted by different research groups, providing emphasis on different aspects.

Brodlie et al. [BAL12] provided an analysis of uncertainty in data visualization. They started with an uncertainty definition and sorted visualization approaches along different types of data. Potter et al. [PRJ12] strived for a taxonomy of uncertainty visualization of scientific data. Followed by that, Bonneau et al. [BHJ*14] presented a STAR on uncertainty visualization which forms a basis for Dwyer et al. [JED*20] to build an online browsing tool to explore several uncertainty-aware visualization approaches. Here, uncertainty visualization approaches were classified based on the underlying data. Olston [OM02] presented a STAR report regarding the visualization of bounded uncertainty. In their paper, common visualization methods for bounded uncertainty are discussed, whereas Hullman et al. [HQC*19] presented a STAR report targeting the evaluation of uncertainty visualization. All these works have in common that they do not focus on medical imaging. As the medical domain provides a unique setting in terms of uncertainty quantification, we aim to provide a state-of-the-art report for medical imaging.

State-of-the-art analysis in the medical domain has been conducted on different topics, such as multi-modal visualization [LSBP17], visualization tools [YCMA12], and flattening-based visualization techniques [KMM*18]. Their findings show that the specific application of medical imaging results in special requirements that need to be considered in the respective research field. We aim to apply this principle to the presented state of the art analysis.

Ristovski et al. [RPHL14] provided a taxonomy of uncertainty in medical visualization. In their work, all sources of uncertainty in the medical application were collected, mathematically described, and examples for visualization approaches were given. Although this provides a valuable starting point for the presented work, the work lacks an extensive description of already existing uncertainty-aware medical imaging approaches. We apply the provided taxonomy to the sources of uncertainty in medical imaging and utilize this as a starting point of the presented work. In contrast to the mentioned work, we provide lists of available approaches in each category of the taxonomy. In addition, the work of Ristovski et al. covers only work up until 2013. Since then, there has been a variety of attempts to tackle uncertainty in the medical imaging area which we would like to consider in this work.

Paper Selection Criteria In this STAR we aim to present uncertainty-aware visualization approaches in medical imaging from the visualization field as well as the medical field. To achieve this, we investigated different venues and companies on the intersection between medical imaging and visualization. The goal was to obtain related work that has been published in the field of medical imaging that considers visualization approaches related to uncertainty analysis.

We searched conferences and journals related to *IEEE Transactions on Visualization and Computer Graphics*, *IEEE Transactions on Medical Imaging*, *Computers & Graphics*, *Eurographics Digital Library*, *Computer Graphics Forum*, *Uncertainty Quantification in Scientific Computing* as well as general search platforms, such as *Google Scholar* and *Springer Link*. We excluded further venues from the medical field or uncertainty analysis as we aimed to focus on the visualization aspect of the presented work.

The queries we executed are a composition of two search terms. The first part of the query relates to uncertainty visualization. Here, we searched for *uncertainty-aware visualization*. We also searched for related terms, such as *sensitivity analysis*, *ambiguity analysis*, and *uncertainty analysis* to deal with the ambiguity of the term uncertainty. The second part of the query relates to *Medical Imaging* and all subgroups of the topic that we have listed in this work (see Figure 2). In addition, we searched for applications of medical imaging, such as *diagnosis*, *intraoperative support*, *treatment planning* and *education*. In particular, we utilized the Cartesian product of the following query term sets to search for adequate results.

1. Uncertainty-aware Visualization | Uncertainty Visualization | Uncertainty Analysis | Sensitivity Analysis | Ambiguity Analysis, Variability | Variation
2. Medical Imaging | Medical Imaging subcategories (Figure 2) | Diagnosis | Intraoperative Support | Treatment Planning | Education

Resulting from those queries, 250 research papers were obtained, filtering out methods that do not fulfill the following requirements:

1. Medical image data as an underlying dataset (at least with one demonstrated example)
2. Uncertainty visualization in at least one of the three defined steps of medical imaging

At this point, we want to highlight that we explicitly exclude work that covers image-based clinical studies. Although these studies work with medical image data as well, they typically do not follow the classic medical imaging pipeline as outlined in this manuscript. These studies make use of the presented approaches rather than introducing them. In this context, we want to highlight that the outcome of the studies is highly influenced by the chosen imaging methods but inclusion in this STAR report would exceed the current scope.

In addition, the clear relation between statistical, ensemble, and parameter space visualization and the presented topic is obvious. Here, we are not able to cover this relation in the given format.

STAR Organization In this work, we start with a general description of the medical imaging pipeline in order to define all important terms that are used throughout the manuscript (see section 2).

After that, we demonstrate the role of uncertainty in medical imaging (see section 3). Here, we start with important terms regarding uncertainty (section 3.1) and show which sources of uncertainty can occur in the medical imaging pipeline. We utilize the taxonomy of uncertainty visualization by Ristovski et. al [RPHL14], to develop a taxonomy of uncertainty in medical imaging (section 3.2). Based on this knowledge, we determine requirements that need to be fulfilled in order to provide an uncertainty-aware visualization for medical imaging (section 3.3).

To provide an easy-to-understand classification of existing uncertainty-aware medical imaging approaches, we aim to utilize the steps of medical imaging as the first level of distinction in the reviewed research papers. Here, an uncertainty-aware visualization approach is divided into one of the phases **Image Acquisition**, **Image Transformation**, and **Image Visualization**, as shown in section 4. A specific approach can also be listed in multiple categories if it is captured by the respective technique. Please note that we will keep the introduced color scheme throughout the entire manuscript (including tables and figures) to provide an easy-to-follow structure. We want to highlight that uncertainty visualization can occur in any of the medical imaging phases as the visualization may not solely address the underlying data but also the uncertainty of the acquisition process as well as the transformation. In contrast to the visualization phase itself, we will focus on the visualization approaches utilized to visually encode uncertainty. **Image Acquisition** (see section 4.1) will be divided into different acquisition techniques commonly used. Along with each technique we provide existing uncertainty quantification approaches and show the found visualization approaches. **Image Transformation** (see section 4.2) will be separated into different processing algorithms commonly used in this category. Uncertainty processing approaches in each category will be discussed and available visualization approaches will be demonstrated. **Image Visualization** (see section 4.3) techniques will be divided along different visualization styles. These can vary based on the visualization paradigm used to create a specific visualization

Besides uncertainty-aware visualization approaches that are targeting a specific aspect of the medical imaging pipeline, there exist uncertainty-aware visualization approaches that aim to provide an application of these techniques to medical tasks. Preim et al. [PB14a] classified medical applications into four subgroups that will be used in the remainder of this report to provide a state of the art in uncertainty-aware visualization approaches in **Medical Imaging Applications** (section 5).

The performed state-of-the-art analysis will be discussed in section 6. Here, we check the presented approaches against the defined requirements and show how single steps of the image processing pipeline can be formed into an entire image processing pipeline. Remaining open problems will be summarized in section 7.

2. Medical Imaging

Medical imaging is concerned with the analysis, visualization, and exploration of medical images [PB07]. Medical imaging comprises three different steps, as shown in Figure 1. Each of these steps can be implemented differently, leading to further categorization of medical imaging approaches. An overview is shown in Figure 2. These groups of techniques will be briefly explained in the following.

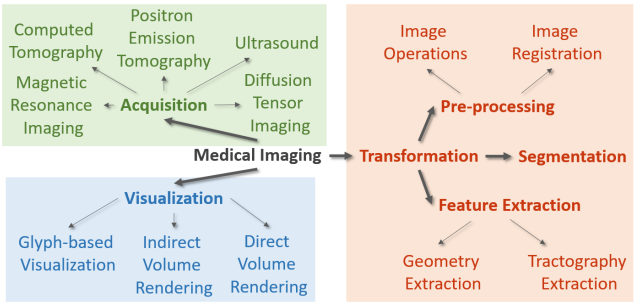

Figure 2: *Medical imaging and its subcategories examined in this state of the art analysis. The main categories are **Image Acquisition**, **Image Transformation**, and **Image Visualization**.*

2.1. Image Acquisition

Image acquisition techniques include Ultrasound, Computed Tomography, Magnetic Resonance Imaging, Diffusion Tensor Imaging, and Positron Emission Imaging [Nud86]. There exist more image acquisition techniques, especially in the context of endoscopy, but we limit the considerations in this work to the most prominent image acquisition techniques that are based on reconstruction processes as shown by Atabo et al. [AU19]. Depending on the acquisition technique, the generated image holds different properties. They can be 2D/3D, time-dependent, and the number of scalars per grid point can vary.

Ultrasound Ultrasound imaging is based on the interaction of sound waves with living tissue producing an image of the tissue [Coo01]. It is usually a handheld device where clinicians can get a first impression of the tissue or an organ that needs to be examined. Ultrasound images can be acquired in real-time resulting in either 2D, 3D, or 4D images for each time step. Based on the underlying physics in the image acquisition process, ultrasound is mainly suitable for imaging soft tissues (for example tendons, vessels, and organs).

Computed Tomography Scans (or X-Ray Scans) are based on the principle that the density of tissue can be measured by the calculation of the attenuation coefficient. The X-ray emitter discharges monochromatic photons that can be measured and computed back based on a model describing the number of photons that can be passed through tissue [LFM*15]. It is a widespread technique in clinical daily routine that can be utilized in a very versatile way for organ inspection and to determine proper treatments. This technique results in a 3D image containing density values. Depending on the chosen imaging parameters, CT allows for the differentiation of structures, such as bone and contrast-enhanced blood vessels.

Magnetic Resonance Imagining (MRI) is based on a strong magnetic field that forces hydrogen protons in the body to spin out of equilibrium. When the magnetic field is turned off, MRI sensors are able to detect the energy released as the protons realign with the magnetic field [HB97]. Intensities in MRI data are not standardized. MRI data often results in an inhomogeneous gray level distribution which requires pre-processing of the data. In addition, intensity values vary depending on scanner vendor and clinic. This imaging technique is very helpful in indicating the perfusion in different types of tissues, for example.

Diffusion Resonance Imaging (DTI) is based on the same principle as MRI. In addition, mathematical models are utilized to compute the diffusion of water molecules to generate contrast in MR images. This allows the mapping of the diffusion process of molecules, mainly water [LBMP*01]. DTI is utilized to assess the deformation of white matter by tumors, for neurosurgical planning (such as the removal of a tumor), and for the diagnosis of brain pathologies, such as Alzheimer's disease and multiple sclerosis. DTI is often considered as part of MRI, but in this survey, we want to highlight the challenge of quantifying and communicating uncertainty in tensors which differs from scalar values. Therefore, we separate DTI and MRI uncertainty visualization techniques in the remaining manuscript.

Positron Emission Imaging (PET) is an imaging technique that uses radioactive substances to visualize and measure metabolic processes in the body [SMS*18]. These images usually show a time series of two-dimensional images. This is often used to obtain an image of active areas, such as activated regions in the brain.

2.2. Image Transformation

Image transformation techniques are plentiful with lots of options, such as image correction, image registration over region definition, and geometry extraction algorithms [CLP18]. In general, it describes the analysis and processing of images [Jä08]. Medical image transformation [Ban08] can be roughly separated into the categories image pre-processing (such as contrast enhancement), image segmentation, and feature extraction (such as extraction of shapes of organs).

Image Pre-Processing Image pre-processing operations can be divided into different categories ranging from edge detection over image enhancement techniques to image registration. In many medical applications, it is important to consider multiple image datasets of one patient to identify diseases or develop proper treatments. These time-series images need to be correlated, referring to Image Registration. Image Operations on the other hand, summarize all types of operations that output a manipulated image. These operations can be performed in different ways such as with edge detection, image enhancement, or color correction.

Image Segmentation is probably one of the most important tasks in medical imaging. Here, the goal is to define regions that represent structural components of the human body [PXP00, BZK03]. Image segmentation is required in nearly every medical imaging pipeline as the definition of regions is required for most medical tasks, such as organ detection, computation of sizes, or detection of anomalies.

Feature Extraction. In many cases, it can be helpful to transform a medical image or parts of it into another data format to understand specific physical connections in the human body. A prominent example is Surface Extraction where segmented parts of the medical image are represented by a surface. Another example is Trajectographies, usually based on the diffusion information in MRI or DTI. Here, paths are computed that follow the diffusion of water.

2.3. Image Visualization

Image Visualization is a widely researched field as it allows medical doctors to review medical images quickly, determine a diagnosis, and decide on a proper treatment plan [LML*07]. Visualization of medical images can be accomplished by a variety of visualization methods, e.g. volume rendering, geometry rendering, or a combination thereof [HFPN90]. Also, each of these techniques can make use of different visual variables, such as color-coding, size and shape of an object, or motion [Bur11].

Direct Volume Rendering is a family of algorithms to visualize three-dimensional image data. Volume rendering requires every sample value to be mapped to opacity and a color. This mapping is accomplished using a transfer function.

Indirect Volume Rendering is based on an indirect surface mesh representation. This mesh is either generated by extracting an isosurface from the original volume data or by transforming a segmentation result [PB14b].

Glyph-based Visualization approaches are a set of depicted properties that are encoded by a collection of visual objects [BKC*13]. Glyphs are a prominent tool to represent tensors or cases where multiple properties need to be visually encoded.

2.4. Applications

Typical applications for medical visualization are educational purposes, diagnosis, treatment planning, and inter-operative support. Here, medical visualization is intended to support clinicians during their daily tasks. In the following, we aim to describe these categories briefly for further reference.

Diagnosis refers to the decision about the exact character of a disease. In particular, diagnosis is concerned with the severity of a disease as well as the extent and precise location of pathology. In the given context it refers to surgery, radiation treatment, and interventional radiology. As this manuscript focuses on medical imaging, it does not include drug treatment or psychiatric treatment, as image data is not relevant in these cases. This process is often aided by medical imaging, as this technique holds the possibility to examine different tissues and their location. Here, medical doctors aim to use medical imaging in order to determine anomalies and derive a diagnosis based on them [RFCL16].

Treatment Planning is an important application for medical imaging. Here, a proper plan for the treatment of a specific disease needs to be derived. Medical imaging can be of massive help in any treatment planning where tissue needs to be examined, as well as in spatial procedures, such as surgeries or radiation. Here treatment steps need to be determined properly [KAS97].

Intraoperative Support is required in many procedures in the medical context. Especially surgeries that need to be processed and hold a high potential for complications require an assistance mechanism. During these tasks, medical imaging can aid in determining complications or aid in adjusting the current procedure [ASV*18].

Education is an important application of medical visualization. When starting with medical education, students first need to study anatomical structures and compositions of the human body before they can start treating patients. Here, visualization plays an important role in creating a first understanding of the human body and potential diseases [SFP*00].

3. The Role of Uncertainty in Medical Imaging

We have shown that medical imaging consists of multiple steps that can be implemented differently. This process can introduce various sources of uncertainty. In this section, we aim to clarify the term uncertainty, derive a taxonomy of uncertainty in medical imaging, and determine requirements for a successful uncertainty-aware visualization for medical imaging.

3.1. Definition, Description, and Quantification of Uncertainty

Independent from the data source, datasets are usually acquired by measuring or simulating phenomena. This creates data points that can be related to each other.

Let $c \in (-\infty, \infty)$ be a measure and c^* be the true value of some measurand. When performing the actual measurement, the result will be $c^{'}$. c^* and $c^{'}$ may be the same value, but usually deviate in reality due to a variety of effects. As a result, the error e of the performed measurement can be defined as the difference between the measured value and the true value of the measurand [BJ15]. This means: $e = |c^* - c^{'}|$. As a consequence, the quantification of an error requires a ground truth that clearly shows the difference between the actual value and the measured value (Figure 3). In contrast to this, the uncertainty is the quantification of the doubt about the measurement result [HDF10]. This doubt can originate from a variety of effects such as [BHP15]:

- incomplete definition of the measurand
- the imperfect realization of the definition of the measurand
- non-representative sampling
- inadequate knowledge of the effects of environmental conditions
- imperfect measurement of environmental conditions
- personal bias in reading analog instruments
- finite instrument resolution or discrimination threshold
- inexact values of measurement standards, reference materials, and parameters
- approximations and assumptions incorporated in the measurement method and procedure
- variations in repeated observations of the measurand under apparently identical conditions

These effects can have different *categories*: uncertainty based on the underlying model (epistemic uncertainty e) or statistical uncertainty resulting from variations in the measurement result when running an experiment multiple times (aleatoric uncertainty a). Here, a model refers to a computational description that tries to map physical dependencies as adequately as possible. Naturally, a model is never complete, as the knowledge about the physics surrounding us is not complete as well. In most cases, aleatoric uncertainty is usually the type of uncertainty that is requested to be visualized in order to enhance a decision-making process in a given application [PRJ12].

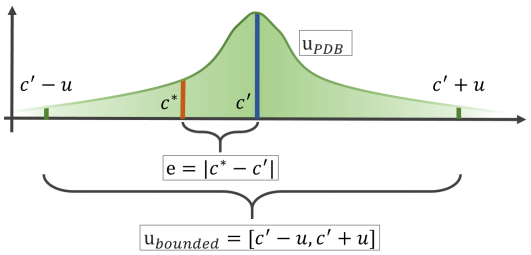

Figure 3: *Error vs Uncertainty. Errors can be measures according to a ground truth whereas uncertainty needs to be quantified.*

There is no unique definition of how to compute uncertainty. In fact, arbitrary functions can be considered to achieve uncertainty quantification. In this work, we will consider the two most popular uncertainty quantification methods found in the literature: *bounded uncertainty* and *probabilistic uncertainty*.

In many cases, uncertainty is described as a boundary around the measurand [OM02]. This defines an interval around the measurand that can be defined as: $u_{range} = [c^{'} - u, c^{'} + u]$. This description of uncertainty is chosen when the focus is not on how the occurrences of a measurand are distributed. Instead, it is important to know the limits in this variation [BBC87].

Another popular description of uncertainty utilizes probabilistic distribution functions [LvB17]. These functions allow describing the probability density of a measurand to be located at an arbitrary point in some space. Here, the measurand usually defines the most probable location of the true value that was captured. The most prominent choices of probabilistic distribution functions are Gaussian distribution functions but in general any distribution can be used to express uncertainty.

As mentioned above, there are many different uncertainty quantification approaches. This leads to the *uncertainty quantification problem*. This problem can be approached from two different sides: *forward uncertainty quantification problem* and *backward uncertainty quantification problem* [Hel08]. In the following, we list examples in each category that will become relevant in the performed state-of-the-art analysis.

Forward uncertainty quantification works on the basis of the propagation of input data uncertainty. As a result, the uncertainty of the output of a system can be quantified. These approaches aim to capture the variance in a measure and accumulate it throughout a sequence of computations. Forward uncertainty quantification techniques use different types of stochastic sampling strategies, such as Monte Carlo sampling. An overview is provided by Lin et al. [LEE12]. Forward uncertainty quantification is usually utilized to quantify *epistemic* uncertainty. The presented techniques in this state of the art report include:

Sources of Uncertainty	Type	Dimensionality of Event	Category	Description of Event
Positional uncertainty	a	3D	numerical	discrete
Pixel/voxel value uncertainty	a	nD	numerical	discrete
Incompleteness of Data	a	nD	numerical	discrete
Model inaccuracy	e	3D	spatial/volumetric/numeric	discrete/continuous
Model incompleteness	e	3D	spatial/volumetric/numeric	discrete/continuous
Parameter/boundary condition uncertainty	a/e	nD	numerical	discrete
Rasterization uncertainty	e	2D/3D	numerical	continuous
Perceptual and cognitive uncertainty	e/a	3D	binary	continuous
Decision making bias	e/a	3D	binary	continuous

Table 1: *Taxonomy of Uncertainty in Medical Imaging. Sources of Uncertainty are listed and origin, dimensionality, type of event, and description of event are listed. Color-coding indicates which source of uncertain occurs in which step of the medical imaging pipeline.*

- Stochastic based sampling
- Monte Carlo sampling
- Markov Chain Monte Carlo model
- Random walks
- Bootstrapping
- Bolzmann distributions
- Time-variations

Backward uncertainty quantification aims to determine the difference between the experiment and the mathematical model. These techniques are usually utilized to capture *aleatoric* uncertainty. This group of algorithms is very heterogeneous. For further detail on the individual methods, we would like to refer to the book by Smith [Smi13]. Backward uncertainty quantification approaches that are utilized by the visualization approaches presented in this work are the following:

- Regression analysis
- Analytical quantification
- Gaussian noise estimation
- Bayesian approaches
- Maximum likelihood estimation
- Subset expectation maximum reconstruction
- Probabilistic deformable regression
- Belief theory [Cat03]
- Kullback-Leibner divergence
- Kinetic modeling

All these approaches aim to provide a measure that is able to express how close the captured measurand is to the underlying computational model by trying to solve an equation, set of equations, or reach some minimum of an optimization procedure.

3.2. Taxonomy on Uncertainty in Medical Imaging

As previously outlined, medical imaging consists of multiple steps. Ristovski et al. [RPHL14] put a lot of effort into creating a taxonomy of uncertainty in medical visualization. Their classification provides a list of sources of uncertainty where random fields (RF) are used to describe each of these sources. This enables the utilization of an arbitrary uncertainty description function. A source of uncertainty is described as an event that can have a *dimensionality*, a *category*, and a *description*. The dimensionality describes a number larger than zero capturing the space that is required to describe a type of uncertainty. The category describes the mathematical instance that is present in each point of the defined space and the description defines whether the events occur in a discrete or continuous fashion. In the following, we aim to provide an application of the taxonomy by Ristovski et al. to medical imaging. In addition to their classification, we also provide a separation of each source of uncertainty into the steps of medical imaging as well as a separation of the mentioned sources of uncertainty into aleatoric or epistemic uncertainty. Table 3.2 provides an overview of the determined taxonomy which will be explained in the following.

Image Acquisition can introduce three different types of uncertainty, which will be explained in the following.

Positional uncertainty is a source of uncertainty that occurs in the image acquisition step. Here, a position of an acquired image in space can vary. This is especially an issue when considering Ultrasound Imaging where the device is hand-held and each time the device is used, the position needs to be acquired. In addition, positional uncertainty can occur when examining surfaces that represent medical structures such as vascular systems. At last, positional uncertainty can be an issue when considering tractography. This uncertainty is crucial when it comes to image registration tasks where multiple images need to be aligned to one point in space. Positional uncertainty is an aleatoric type of uncertainty that can occur as a three-dimensional event where the events are numerical and discrete.

Pixel/voxel value uncertainty occurs in any type of medical imaging. The process of capturing signals, independent of their form, is always affected by uncertainty. Especially in the medical field, where structures in the human body are captured and there exists no direct correlation between the captured images and the ground truth, this is probably the most frequently occurring and influencing form of uncertainty. Due to the numerous effects that influence this type of uncertainty, it can be described as an nD event with numerical and discrete events.

The incompleteness of Data is an effect that occurs due to the discretization of data when capturing an image. Medical imaging is always restricted to a specific resolution that depends on the device constraints and other physical restrictions. This type of uncertainty is aleatoric and results in nD events that are numerical and discrete.

Image Transformation techniques can introduce sev-

eral sources of uncertainty into the medical imaging pipeline [MPG*16].

Model inaccuracy is a type of uncertainty related to the mathematical description of a model. Models typically simplify physical behavior and can therefore not be a perfect replication of reality. This type of uncertainty is epistemic and results in 3D events that can, depending on the model, be spatial, volumetric, or numeric and with discrete or continuous events.

Model imprecision is highly related to model inaccuracy and origins from approximations in computation that are necessary to be able to compute physical behavior. Therefore, the events of model inaccuracy result in 3D events with spatial, volumetric, or numeric events with discrete or continuous descriptions.

Parameter/boundary condition uncertainty refers to the parameter and boundary conditions that are used to implement and run a model. As models usually show a snapshot of reality, they are implemented as closed systems where parameters and boundary conditions need to be determined. This is often accomplished experimentally, but most of the time it is still not clear if a chosen parameter is perfect or an optimal choice. This uncertainty results in nD events (depending on the number of parameters) with numerical and discrete events.

Image Visualization holds three different types of uncertainty.

Rasterization uncertainty refers to the problem when the data need to be visualized. Here, the screen that shows the resulting visualization deploys a discretization typically of lower resolution than the full complexity of the visualization model. Depending on the desired visualization (2D or 3D), the resulting event has the same dimensionality, holding numerical and continuous events.

Perceptual and cognitive uncertainty is related to the user that interacts with the provided visualization. Humans can have very different perceptual interpretations even though they all interact with the same type of visualization. This uncertainty results in 3D events that are binary and continuous.

Decision-making bias is also highly related to the user of a visualization itself. When dealing with medical image data on a daily basis, a personal decision-making bias can form that affects the way a user interacts with a visualization. This uncertainty is epistemic and aleatoric and can be described as 3D events of a binary type and a continuous description.

As shown in this section, sources of uncertainty can be found along the entire medical imaging pipeline. They do not need to occur in all cases but at least one of them likely occurs. As uncertainty can highly affect the decision-making process in medical imaging, uncertainty needs to be properly communicated.

3.3. Requirements for Uncertainty-aware Visualization in Medical Imaging

As shown before, uncertainty is an important issue that needs to be included in visualization approaches in medical imaging. The development of the taxonomy of uncertainty in medical imaging has also shown that uncertainty adds at least one random field to the originally captured image data, resulting in an increase of complexity that needs to be communicated. In this section, we list the requirements that need to be fulfilled in order to provide a suitable uncertainty-aware visualization in medical imaging.

When considering the medical field, there exist a variety of requirements that need to be fulfilled that originate from legal restrictions [MSH*20]. These restrictions are not specific to uncertainty-aware visualization itself.

We discussed all requirements with our medical collaborators and searched for the most important in the given context. The medical collaborators are all working in clinics and include a neurologist, a dermatologist, and a surgeon. We asked all collaborators to rate each requirement from 1 (not import) to 5 (very important). Here, we obtained 3 requirements that have been rated with 4 and 5 from all three clinicians. As a result, we restrict the formulated requirements for uncertainty-aware visualization approaches to the visualization design itself while explicitly considering the special needs in medicine that have been proposed by Preim and Bartz [PB07].

In this context, the main goal when designing uncertainty-aware visualization for medical imaging can be summarized as follows:

- **R1** Show the original dataset
- **R2** Show the related uncertainty
- **R3** Keep the cognitive load minimal

We would like to refer to these challenges throughout the following state-of-the-art analysis.

Here, **R3** is the most critical requirement. Clinicians usually use a very specific visualization approach to review medical image data. This technique, referred to as slice-by-slice reviewing, is consistently trained in medical education and the standard tool to review medical images [FP17]. The inclusion of this technique is highly beneficial in order to ease the use of a novel visualization technique in medical imaging as users can correlate the visualization with a known standard.

We are aware that the formulated requirements are very general. This is due to the fact that we aim to cover a variety of approaches and applications in this work which would raise further requirements by themselves. To achieve unification, the presented requirements are used.

4. Uncertainty-aware Visualization in Medical Imaging

In this section, we aim to give a state-of-the-art report of available visualization approaches in uncertainty-aware medical imaging. The approaches will be separated into three topic areas: **Uncertainty-aware Image Acquisition**, **Uncertainty-aware Image Transformation**, and **Uncertainty-aware Image Visualization**.

4.1. Uncertainty-aware Image Acquisition

Medical imaging techniques are very versatile, creating images of different dimensionalities (2D, 3D, time-varying, scalar, or tensor values) that may contain a variety of values in each image component (scalars and tensors). The process of capturing this data is affected by uncertainty, which can be quantified and visualized.

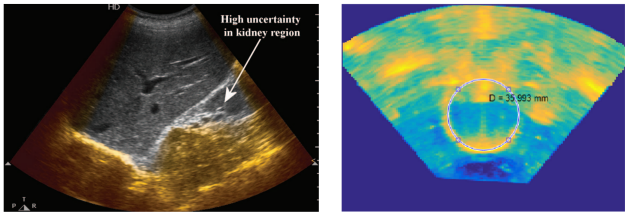

(a) (b)

Figure 4: *Uncertainty-aware visualization of Ultrasound image data. a) Confidence Map in 2D Ultrasound while observing a kidney. Chroma indicates high certainty of the captured image [ZBDH*15]. b) Uncertainty quantification of 3D Ultrasound by measuring the time variation. Yellow indicates areas with high uncertainty [LBdJ18].*

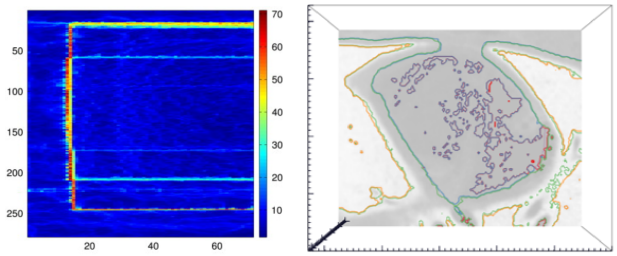

(a) (b)

Figure 5: *Uncertainty quantification approaches for Computed Tomography Scans. a) Stochastic uncertainty quantification in CT scans [HLF14], where red indicates high uncertainty. b) Embedded iso-surface visualization of multiple analytical uncertainty quantification approaches [GAH*17]. Areas that show differing uncertainty behavior are separated by lines using various colors.*

4.1.1. Ultrasound (US)

Hellier et al. [HCMC10] presented a methodology that helps identify the uncertainty in ultrasound images by *estimating the shade* during the time of use mainly in the prostate examination. It is based on the assumption that signal rupture between different ultrasound images indicates uncertainty. This work does not provide a visualization approach for the quantified uncertainty. Instead, Hellier et al. corrected the input ultrasound image according to their uncertainty quantification.

Berge et al. [ZBDH*15] presented confidence maps that visually indicate the trustworthiness of image points by using a colormap, as shown in Figure 4(a), when reviewing a kidney. Here, chroma color indicates areas with high uncertainty. The confidence map is defined as the solution to a *random walk's equilibrium problem* using ultrasound-specific constraints. This methodology was initially introduced by Karamalis et al. [KWKN12].

Stevens et al. [LBdJ18] presented an uncertainty quantification of 3D Ultrasound images based on *time-variations*, as shown in Figure 4(b). The method works based on the assumption that overly drastic changes between images in a time series suggest uncertainty.

Gueziri et al. [GML14] presented a visualization to cover the positional uncertainty of an ultrasound device. Usually, these devices are handhold by the user which can result in distortion of the resulting image. The computation is based on *target registration errors*. Gueziri et al. incorporated this uncertainty into the image reconstruction process to create an awareness of this effect.

4.1.2. Computed Tomography (CT)

Howard et al. [HLF14] utilized a *stochastic sampling* approach to quantify the uncertainty in acquired CT scans. Their goal was to express the value of the uncertainty captured in CT scans. Here, a rainbow color map is used to indicate areas in the image that are uncertain, as shown in Figure 5(a).

Tian et al. [TS16] presented an uncertainty quantification approach that aims to measure quantum noise in clinical body computed tomography. To accomplish this, a *regression analysis* was utilized and the uncertainty was represented in a separate visualization of noisy voxels. In addition, this approach allows us to correct the input images by removing voxels in the image that are uncertain.

A neural network approach provided by Rheinhold et al. [RHH*20] estimates the uncertainty captured in CT scans. The method is based on *Bayesian neural networks* that can output the uncertainty of a computational prediction. This quantification is shown as a separate colormap.

Gillmann et al. [GAH*17] provided a visual analytics approach to examine a high-dimensional uncertainty space of CT scans. Here, multiple uncertainty quantification based on *analytical quantification approaches* were utilized and visualized by using isosurfaces that are included in the slice-by-slice reviewing procedure. Figure 5(b) shows an example of this approach.

4.1.3. Magnetic Resonance Imaging

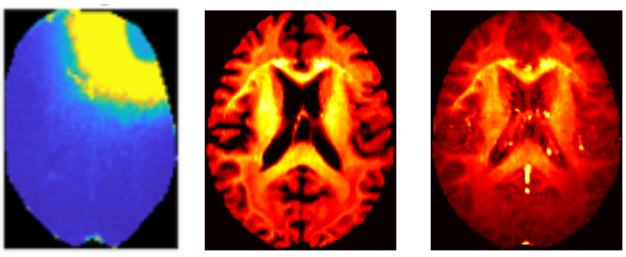

(a) (b)

Figure 6: *Examples of uncertainty quantification algorithms for MRI. a) Uncertainty quantification using Bayesian neural networks [GDP*20]. Yellow indicates areas with high uncertainty. b) Uncertainty Quantification using Markov Chain Monte Carlo Methods [HFSR19]. The left image shows the mean value whereas the right image represents the standard variation. In both images, yellow areas indicate high values.*

Edupuganti et al. [EMVP19] provided a list of statistical uncertainty quantification techniques for MRI. It includes *Monte Carlo sampling*, *Stein's Unbiased Risk Estimator (SURE)*, and *Gaussian noise with density compensation*. In this methodology, the resulting uncertainty measures are visualized by colormaps.

Bayesian neural networks can be utilized for the reconstruction of MRI as shown by Glang et al. [GDP*20]. As a side effect, these networks output an uncertainty map, as shown in Figure 6(a).

Harms et al. [HFSR19] derived an uncertainty quantification of MRI using either *Maximum Likelihood Estimation (MLE)* or *Markov Chain Monte Carlo* methods. The resulting mean and standard deviation expressing the uncertainty when using MLE of the MRI are shown in Figure 6(b).

In addition to the classic MRI, functional MRI (fMRI) can measure brain activity within areas of the captured images. These functional areas can be computed by the detection of changes associated with blood flow. This technique is based on the fact that blood flow and neuronal activation are coupled [HSM08]. Croci et al. [CVR19] utilized the *convection-diffusion–reaction equation* in order to develop an uncertainty quantification. This was achieved by utilizing stochastic modeling and random variables.

4.1.4. Diffusion Tensor Imaging

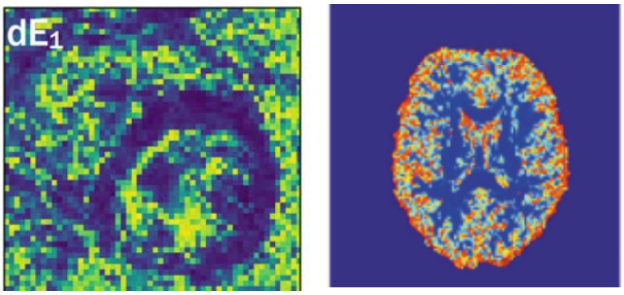

(a) (b)

Figure 7: *Uncertainty quantification of Diffusion Tensor Imaging. a) Uncertainty quantification using bootstrapping [AMME18] where yellow indicates high uncertainty. b) Uncertainty quantification using Markov Chain Monte Carlo Model [BWJ*03]. Red indicates areas with high uncertainty.*

Aliotta et al. [AMME18] presented a *bootstrapping* algorithm that creates a probability distribution based on two captured DTI scans. Based on this procedure, the uncertainty of the original DTI, as well as the uncertainty of the resulting eigenvectors, can be determined. Figure 7(a) shows the resulting uncertainty of the first eigenvector in a cardiac MRI scan. This approach was extended to *wild bootstrapping* by Whitcher et al. [WTW*08].

Behrens et al. [BWJ*03] applied a *Markov Chain Monte Carlo model* in order to estimate the uncertainty in DTI. An example can be found in Figure 7(b).

4.1.5. Positron Emission Imaging

Kinetic modeling can be used to provide an uncertainty quantification of PET images shown by Saad et al. [SSHM07]. They provide a visualization based on color-coding indicating the uncertainty of the reconstructed PET images. Figure 8(a) shows an example.

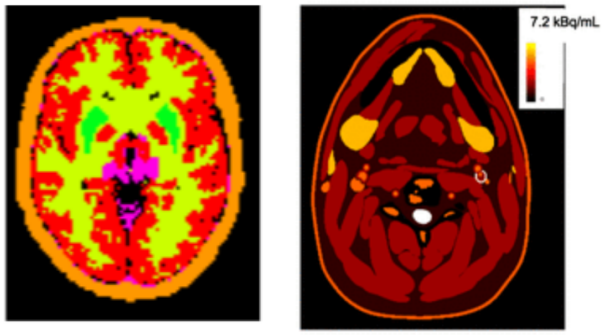

(a) (b)

Figure 8: *Uncertainty quantification of Positron Emission Imaging. a) Uncertainty quantification using kinetic energy modelling [SSHM07] where red and purple indicate high uncertainty. b) Uncertainty quantification using Subset Expectation Maximization reconstruction [HBG*15]. Here, yellow represents high uncertainty.*

Huet et al. [HBG*15] provided an uncertainty quantification of PET using the *Subset Expectation Maximization reconstruction* approach. Their approach is specially designed to target smaller structures, such as vessels, in order to determine the uncertainty when visualizing levels of arteriosclerosis. They achieved this by presenting a color map to the user that indicates the amount of uncertainty per pixel, as shown in Figure 8(b).

Ropinski et al. [NBYR12] compute intra- and inter-model uncertainties and visualize them using a ThemeRiver Metaphor that allows to visually connect several settings of uncertainty. This view is connected with a volume rendering of the original dataset to understand the uncertainties derived in the acquisition process.

Summary: It can be observed that uncertainty analysis is covered in all acquisition disciplines, but Ultrasound and Computed Tomography are the categories that developed the furthest.

4.2. Image Transformation

In the subsequent subsections, we summarize uncertainty-aware image transformation algorithms and will differentiate between image operations that output a processed image and image registration approaches. In this section, we aim to examine uncertainty-aware techniques for image processing and their relation to suitable visualization approaches.

4.2.1. Image Pre-processing

Image pre-processing operations can be divided into different categories ranging from edge detection over image enhancement techniques to image registration. In the following, we summarize uncertainty-aware image processing algorithms and will differentiate between image operations that output a processed image and image registration approaches.

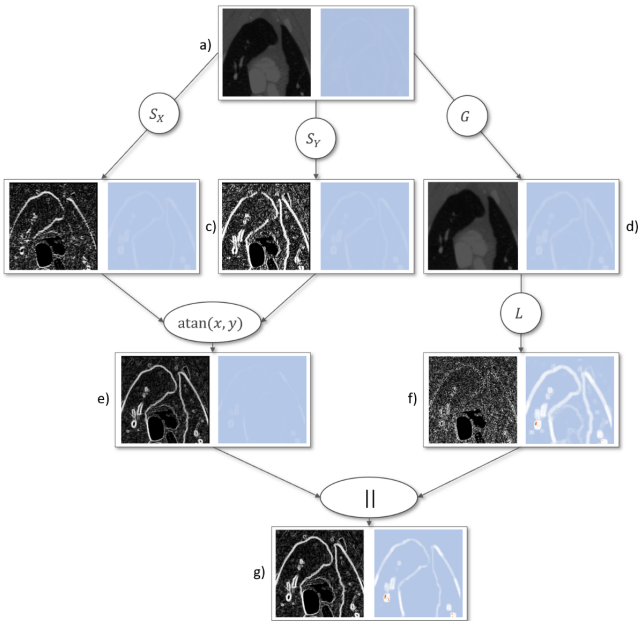

Figure 9: *Uncertainty-aware image operations. Visual pipeline of arbitrary image pre-processing operations by Gillmann et al. [GAH*18]. Individual steps are shown side-by-side to their uncertainty and the computational pipeline is indicated by a graph. Orange shows areas in the images that are highly affected by uncertainty.*

Image Operations When applying image operations, the uncertainty captured in the input image needs to be mapped into the output image. This can be achieved in different ways. In his work, Pal [PAL01] showed that uncertainty quantification and propagation is an important factor that affects image pre-processing operations in different applications.

The first group of uncertainty-aware image operations works on an uncertainty-quantification of the medical image which is propagated by utilizing the uncertainty propagation rules known from physics [Che09].

Pal [PAL01] presents an uncertainty model based on the *analysis of grayness ambiguity* and shows how to propagate this information along an image pre-processing pipeline. Still, this method does not provide a visualization that allows the user to follow the propagation of uncertainty.

Mencattini et al. [MRSS08] presented an image pre-processing pipeline that is adapted by considering an uncertainty quantification of the input image. This quantification can be chosen freely. Although the approach is able to adjust the results in the image pre-processing pipeline according to the underlying uncertainty quantification, it does not provide a visual communication of the uncertainty.

A method for the *Hough transformation* that is able to consider uncertainty information of the input image was introduced by Qiang et al. [JH01]. Hough transformations map the image space onto a selected feature space, where the degree of fitting can be extracted. For medical imaging, this allows determining the degree of similarity of structure shown in an image to a requested feature. Their method showed that the results of a Hough transformation can be significantly improved. This approach as presented is not able to visually communicate the influence of the image uncertainty.

Yi et al. [YHS94] showcased a method that allows the quantification and propagation of arbitrary image uncertainties throughout the image vision pipeline. In their method, they provide a visual representation that demonstrates the current amount of uncertainty in each computational step.

Franco et al. [FCC15] presented a theoretic framework that provides the ability to arbitrarily quantify and propagate uncertainty throughout a medical image processing pipeline. This approach is not coupled with a visualization approach that helps users to navigate through the process.

Gillmann et al. [GAH*18] developed a system that provides quantification of the uncertainty in input images and propagates the computed uncertainty along arbitrary image pre-processing pipelines for US, CT, and MRI images. Their system is guided by a visual representation connecting the computational steps and presenting the development of the overall uncertainty throughout each computational step, as shown in Figure 9.

Alternatively, images can be interpreted as *fuzzy sets*, as shown by Szczepaniak [SLK00]. This allows creating probabilities of image pixels to show a specific object. In the medical field, this relates to the uncertainty of an image pixel representing a specific medical structure. Computational rules are described that determine how to combine several fuzzy sets or how to perform computations based on fuzzy sets in general. This principle is utilized by Chaira et al. [Cha15] to provide an uncertainty-aware image operation.

The operations summarized so far are solely utilized for medical image data that holds one scalar per voxel. More precisely, diffusion tensor imaging cannot directly be processed by these methodologies. Here, the tensors in the DTI need to be either simplified first by tensor measures, such as eigenvalues or norm, or computational approaches that transform tensors into another representation. We will focus on this class of techniques in section 4.2.3.

Image Registration Mahyari et al. [LTAH13] proposed the concept of *Probabilistic Deformable Registration (PDR)* where each voxel of an image is assigned a distribution over the potential displacement vectors. Mahzari et al. utilized uncertainty measures to enhance the standard image registration process.

Bian et al. [BYW*20] proposed a neural network-based approach that is built on Bayesian neural networks to achieve image registration. In this work, the uncertainty output of *Bayesian neural networks* is utilized to quantify the uncertainty in the image registration process. Folgoc et al. [LDCA17] presented a similar approach while relying on sparse Bayesian neural networks. Their result is a heatmap showing the probability of the moving image to be properly based on top of the original image as shown in Figure 10(a).

Risholm et al. [RPSW10] presented a framework to compute the registration uncertainty as well as the most likely deformation that

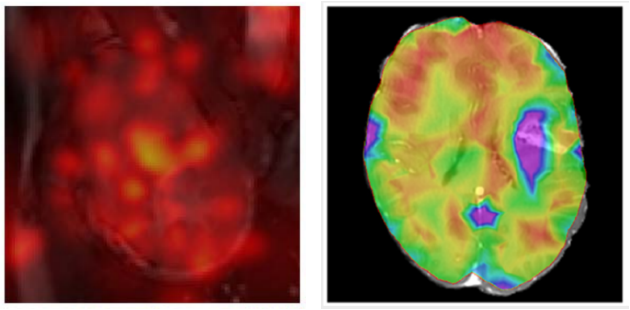

(a) (b)

Figure 10: *Uncertainty-aware image registration approaches. a) Uncertainty-aware image registration using Bayesian neural networks [LDCA17]. Yellow indicates areas where the registration approach is affected by uncertainty. b) Uncertainty-aware image registration using Boltzmann distributions [RPSW10]. Yellow represents areas where image registration is highly affected by uncertainty.*

is required to register image data from the human brain by using *Boltzmann distributions*. In their system, the authors provided a visual representation of the registered image as well as the extent of the deformation, as shown in Figure 10(b). Their visualization approach is specially designed to communicate registration uncertainty during surgery. The technique was refined to deploy color-coding to indicate areas of high registration uncertainty using a colormap [SWGS11].

By considering registration parameters, Yang et al. [YN15] provided an uncertainty quantification based on the *Hessian matrix* that estimates and visualizes the sensitivity of the input parameters in the registration process. Here, they use glyphs to indicate the uncertainty in each image pixel to be correctly mapped.

Schlachter et al. [SFJ*16] provided a visual tool to analyze the accuracy and uncertainty in the segmentation process of deformable image registration. They use a combination of 2D and 3D visualization where color-coding is used to indicate dissimilarities in the registration process.

4.2.2. Image Segmentation

Medical image segmentation is an often-occurring step in analysis procedures. The separation of regions or objects of interest from other parts of the body is of high interest for clinicians as the simplification of a medical image to the region of interest can simplify decisions.

In contrast to classic segmentation definitions where voxels are distributed to segments, *fuzzy segmentations* use probabilities to describe the degree of affiliation to a segment. A review of these techniques can be found in [NMI10]. These methods work on a *fuzzy c-means clustering* algorithm performing an unsupervised segmentation for a predefined number of segments. Still, this type of clustering is sensitive to noise which makes it difficult to use for real-world datasets.

In order to reduce noise sensitivity, different methods [BS09, CCZ07] adapt the fuzzy c-means clustering. These approaches consider the neighborhood of a voxel to decide the segmentation result. Although this increases the applicability of fuzzy segmentation on real world datasets, it is an unsupervised segmentation approach that does not provide a mechanism to insert user knowledge into the segmentation process.

Aside from fuzzy segmentation, Petronella et al. [AVvO*04] created a probabilistic segmentation based on *density measurements* generated from a Magnetic Resonance Imaging (RMI) device.

Graph-cut approaches [KT08] can be extended to result in a fuzzy segmentation [Ada12]. Although this shows the weaknesses of the segmentation result, the user is not able to control the resulting structures. The resulting segments are visualized using color-coding.

Model-dependent segmentation approaches can also be extended in order to achieve an uncertainty-aware segmentation result. Hershkovitch et al. [HR18] presented an approach where models can be overlapped with the target image and the quality of fit between model and image can be determined and visually encoded.

Several approaches describe measures that classify and visualize the classic segmentation results. Benno et al. [LGM*14] utilized *belief functions* that help express the uncertainty in each image pixel. The certainty of the segmentation result is encoded by a colormap.

Al et al. [ATHL14] utilized the *Kullback–Leibler divergence* (or the total variation divergence) to express the uncertainty in the segmentation result. They use color-coding to indicate pixels that cannot be counted into a specific segmentation class for sure. An example of this approach is shown in Figure 11(a).

Saad et al. [SHM10] proposed an interactive framework that allows users to examine the uncertainty of the segmentation result, as shown in Figure 11(b). The quantification of uncertainty in the segmentation result is based on *Bayesian decision theory*. The segmentation result is shown by utilizing a volume rendering approach that color-codes the uncertainty in the segmentation result.

Some approaches that highlight segmentation defects or uncertainty in the segmentation results are available in the literature as well. Prassini et al. [PRH10] presented an uncertainty-aware image segmentation approach that is based on the *random walker computation*. In their visual framework, they indicate the borders of a segment with a certain probability with different lines as shown in Figure 11(c).

Batra et al. [BUK*10] proposed a visually fuzzy segmentation approach where users can guide the segmentation process. Here, users start marking in the original image in order to guide the segmentation algorithm. The segmentation algorithm computes the certainty for each image pixel based on *geodesic distances*, which is visually indicated in the segmentation process and the user can adapt the scribbling input if required, as shown in Figure 11(d).

Using a multi-modal segmentation approach, Al-Taie et al. [ATHL15] also describe the segmentation uncertainty as well. Their approach is suitable for brain imaging and works on a

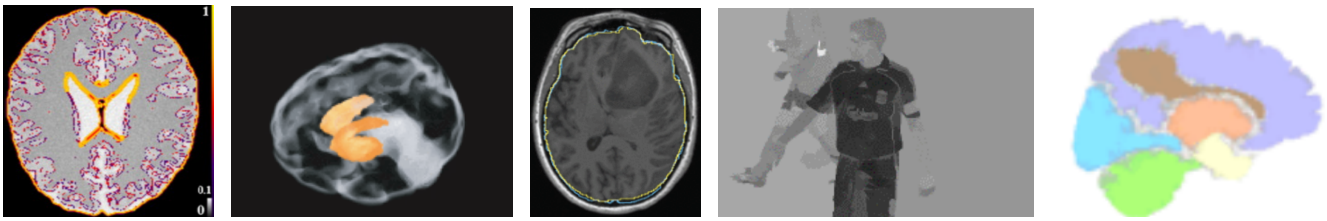

(a) (b) (c) (d) (e)

Figure 11: *Uncertainty-aware medical image segmentation. a) Image Segmentation using Kullback–Leibler divergence [ATHL14]. Areas that cannot be separated clearly are highlighted in yellow. b) Segmentation result based on belief functions [PRH10] shown by volume rendering. Belief functions aim to capture our belief regarding the location of the true value. In the context of image segmentation, they express the probability of a pixel to be contained in a specific segmentation class. Dark orange indicates areas with high uncertainty. c) Segmentation result based on random walker computation approach [BUK*10]. d) Segmentation result based on random walker computation [SHM10]. Light gray areas indicate an uncertain segmentation approach e) Segmentation based on hierarchical geodesic distances [GPW*19]. Transparent and mixed colors highlight uncertain areas in the segmentation result.*

Kullback-Leibner divergence. In addition to the segmentation output, this approach provides an uncertainty map of the segmentation result.

Gillmann et al. [GPW*19] presented a hierarchical and probabilistic segmentation approach where users can design arbitrary hierarchical segmentation classes and initialize them with seed points. The resulting visualization shows the assigned color of each segmentation node and uncertainty between nodes is indicated by the mixing of colors, as shown in Figure 11(e).

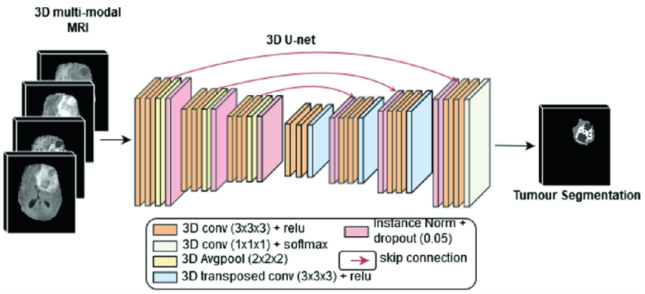

Figure 12: *Uncertainty-aware medical image segmentation using Bayesian neural networks. Based on a U-Net architecture, images can be segmented [MA19].*

Recently, segmentation approaches that are based on neural networks became very popular in medical applications. This is due to the fact that segmentation results can become very accurate when considering neural network approaches and having labeled training datasets. A popular tool to achieve this is so-called U-Nets, as shown in Figure 12. These form a deep convolutional neural network that is able to expand the determined classification in order to restore its location in the original image [RPB15].

A popular tool to express the uncertainty throughout U-Nets is an adaptation that utilizes *Bayesian neural networks*, as shown by Kwon et al. [KWKP20]. These networks are able to output the segmentation result as well as the uncertainty of segmentation results. A popular application for these networks is the lesion segmentation task [JA19]. This is due to multiple effects: first brain lesion datasets are widely available and the detection of a brain lesion is a clear localization task that works as a basis for a U-Net.

Nair et al. [NPAA20] presented a visualization approach that helps examine the segmentation output of neural networks using various uncertainty measures. Here, the segmentation results and the quantified uncertainty are visually encoded in the original image.

4.2.3. Feature Extraction

In many cases, it can be helpful to transform a medical image or parts of it into another data format to understand specific physical connections or other features in the human body. A prominent example is surface extraction where segmented parts of the medical image are represented by a surface. Another example is trajectography, usually based on the diffusion information in MRI or DTI.

Surface Extraction The original surface extraction algorithm known as marching cubes [LC87] is a well-known algorithm. It is based on a selected value that determines the resulting surface elements. Although this algorithm has been successfully applied to many problems, the original algorithm is not able to adapt its value throughout the image to match the desired surface.

Glanznig et al. [GMG09] presented a marching cubes method that is able to automatically adapt its iso-value throughout the extraction process, as shown in Figure 13(a). Here, users can select different types of iso-value generation such as random distributions around a set value or iso-value generation based on image gradients. Still, this process is not guided by a visual approach.

In general, the marching cubes algorithm can lead to degenerated meshes, independent of whether a dataset is affected by uncertainty. Dietrich et al. [DSS*09] inserted surface points into the original surface to preserve topological features.

Pothkow et al. [PWH11] presented a probabilistic marching cubes approach that captures the uncertainty of the resulting geometry. Here, joint distributions of random variables associated with

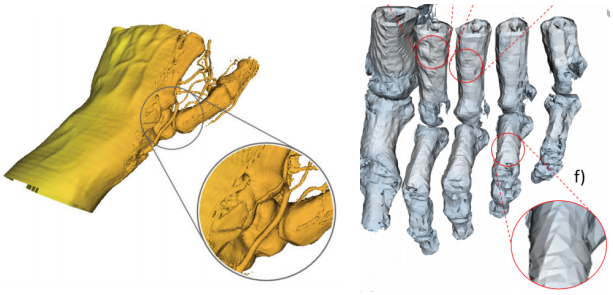

(a) (b)

Figure 13: *Uncertainty-aware geometry extraction in medical imaging. a) Uncertainty-aware geometry extraction through adaptive isovalues [GMG09]. Dark orange highlights areas with high positional uncertainty. b) Uncertainty-aware optimization of the extracted surface using arbitrary uncertainty measures [GWHH18]. White color indicates high uncertainty in the position of the surface.*

the sample locations are utilized to compute level crossing probabilities for cells of the sample grid.

By utilizing an analytical uncertainty model, He et al. [HMH*15] extended the original marching cubes algorithm. They *propagate* this information throughout the marching cubes algorithm. This approach leads to an uncertainty visualization complementing the extracted isosurface.

Gillmann et al. [GWHH18] presented an isosurface extraction algorithm that is based on the classic marching cubes algorithm. Here, the algorithm starts with an isosurface that was extracted by the marching cubes algorithm. For each of the points included in the surface, the algorithm adapts the point position to move the surface into a direction in such a way that the measured uncertainty of the input image is minimized while at the same time trying to preserve the original geometry. The remaining uncertainty is encoded via color-coding of the surface, as shown in Figure 13(b).

Tractography Extraction Tractography is a 3D modeling technique for visually representing nerve tracts and thereby understanding the functionality of the human brain [Mor07]. This method is usually deployed to examine MRI or DTI data. It is based on the measure of the apparent diffusion coefficient at each voxel. Using seed points, a space-path through the field of diffusion coefficients can be computed.

Bornemo et al. [BBKW02] presented a fiber tracking approach that is based on *stochastics and regularization* allowing paths originating in a seed point to branch and return a probability distribution of possible paths. Possible paths can be visualized in the original slice-by-slice view as shown in Figure 14(a).

Friman et al. [FFW06] utilized a *Bayesian stochastic analysis* to compute potential tractography. The resulting computations are visualized in the original slice-by-slice view.

Bootstrapping is a very popular group of approaches to capture the uncertainty in tractography [CFJ*06, Jon08]. This approach is

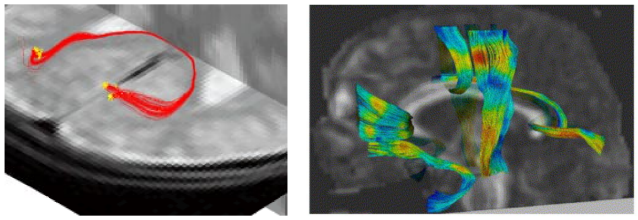

(a) (b)

Figure 14: *Uncertainty-aware tractography in MRI and DTI data. a) Tractography visualization using multiple paths [BBKW02] to indicate variations in the path. b) Uncertainty visualization of potential paths using first eigenvector direction as color-coding [CLH06]. Red shows segments of the path that hold a high positional uncertainty.*

based on random sampling and assigns measures of accuracy to the measured samples. Several approaches utilize bootstrapping to quantify the uncertainty of the tractography and visualize the potential paths. Chung et al. provided a comparison of available bootstrapping approaches [CLH06]. The visualization is normally an inlay of potential paths in the original slice of the image data to provide spatial context. Figure 14(b) shows an example of this approach.

Behrens et al. [BBJ*07] presented a direct extension of probabilistic diffusion tractography to the case of multiple fiber orientations. Their approach is based on *relevance determination* that allows users the online selection of a number of fiber orientations supported by the data at each voxel. These paths are visually encoded in the slice-by-slice visualization.

Descoteux et al. [DDKA09] provided a visual approach to examine variations in tractography. Here, orientation distribution functions (ODF) are modeled using *sharpening deconvolution functions (SDF)*. The resulting tractography is minimized to one path that is color-coded to indicate the strength of geometric variation.

Brecheisen et al. [BPVHR12] used a *Wild Bootstrap algorithm* combined with a *fiber tracking algorithm*. They utilized illustrative rendering to minimize the paths that need to be drawn. Here, surrounding hulls indicate frequently occurring paths.

Summary: This section shows that there exists a variety of image transformation approaches. In addition, each category contains at least one example, where all requirements can be fulfilled.

4.3. Image Visualization

Independent from the visualization of uncertainty measures or the visualization of image pre-processing results, the medical images themselves need to be visualized in order to provide clinicians with powerful decision-making tools. In this section, we will differentiate between direct volume rendering approaches; indirect volume rendering approaches; further visualization techniques, such as flattening-based visualization or illustrative visualization; and visual analytics systems.

4.3.1. Direct Volume Rendering

Volume rendering is a straightforward tool to visualize three-dimensional medical image data.

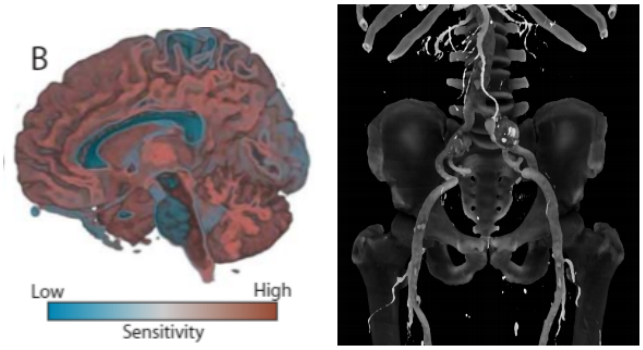

(a) (b)

Figure 15: *Uncertainty-aware volume rendering. a) Volume rendering to encode sensitivity of the input image [Kni08]. Red indicates high sensitivity. b) Ambient occlusion of uncertain anatomical structures [KSE16]. Uncertain structures are shown less opaque.*

Kniss et al. [Kni08] provided a method that uses *two-dimensional transfer functions* to allow the user to select different structures in an image. Here, the methodology allows the use of color transfer functions that indicate the confidence of voxel values, as shown in Figure 15(a). Mia et al. [MCC*20] refined this approach to allow users to express the feature of interest via transfer functions. Here, volume rendering is used to indicate uncertain areas in the resulting volume visualization by distortion.

Lundstroem et al. [LLPY07] proposed an uncertainty-aware volume rendering approach that captures uncertainty through *animation*. The rendering is animated by sampling the domain of probabilistic transfer functions over time, which results in a varying appearance of regions. Contrary to a variety of approaches listed so far, the defined target of providing an easy-to-understand visualization that addresses medical researchers' needs is excellently implemented in this approach. In addition, it contains a strong evaluation, which makes it one of the most remarkable works in this manuscript.

Kroes et al. [KSE16] presented an ambient occlusion approach for direct volume rendering that allows the highlighting of certain structures while utilizing volume rendering, as shown in Figure 15(b). Here, occlusion maps are updated according to the certainty of the input dataset.

4.3.2. Indirect Volume Rendering

Indirect volume rendering refers to the rendering of geometries [ZT03]. Although this section is highly related to section 4.2.3, we distinguish between these approaches as they are not directly related to the source of the geometry that is utilized. We want to separate these topics as geometry extraction methods produce the geometry that needs to be visualized and indirect volume rendering is solely concerned with the visualization of geometry, independent from its source.

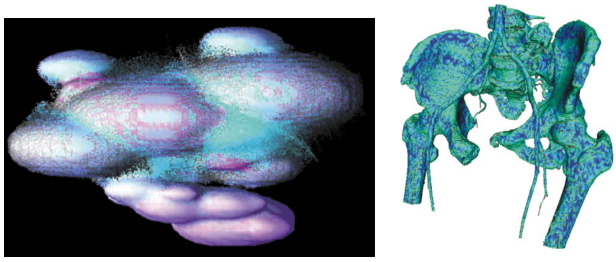

(a) (b)

Figure 16: *Uncertainty-aware indirect volume rendering. a) Indirect Volume Rendering using color-coded point clouds [GR04] where purple indicates surface points with high positional uncertainty. b) Iso-surface representation with uncertainty color-coding for uncertain points included in the surface [Dra08]. Blue shows high uncertainty.*

Rhodes et al. [RLBS03] evaluated different techniques to visually encode uncertainty on isosurfaces. They tested different modes as color-coding, textures, and a combination of these techniques for multi-modal visualization. They found that color-coding is a suitable method to visualize uncertainty on a surface.

Grigoryan et al. [GR04] presented a probabilistic description of points that can describe extracted surfaces. In contrast to marching cubes, solely *points* that represent a surface are extracted. In this method, for each point a probability is computed that encodes how likely it is that this point is part of a surface, as shown in Figure 16(a).

Drapikowski [Dra08] described a model for isosurface uncertainty characterization in medical applications based on geometric features such as *smoothness and curvature*. These features were combined with knowledge of the underlying image structure and the human anatomy to determine the quality of an isosurface. This uncertainty is color-coded into the surface, as shown in Figure 16(b). This is an important issue when designing prostheses that need to fit perfectly onto a bone of a patient.

Gillmann et al. [GWHA18] provided a visual approach to indicate positional uncertainty in extracted surfaces. Here, semi-transparent isosurfaces are utilized to encode potential locations of surface points.

4.3.3. Glyph-Based Rendering

As a DTI dataset contains tensors, a suitable tensor visualization needs to be derived. Here, glyphs are a common visualization tool. Ropinski et al. [ROP11] provided an overview on glyph-based spatial multivariate medical data and highlighted the need for uncertainty-aware tensor glyphs [GRT19].

Jones et al. [Jon03] utilized *cones of uncertainty* that indicate the uncertainty in each voxel of the DTI scans. Here, the cones gain in size when the uncertainty increases. In addition, the cones are oriented such that the tractography direction can be determined.

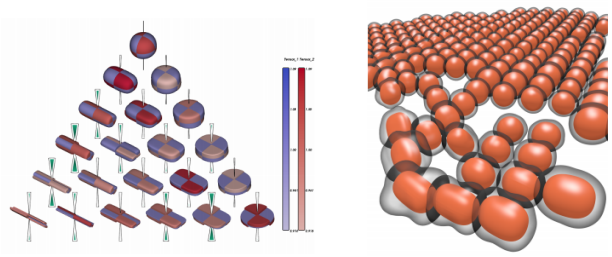

(a) (b)

Figure 17: *Uncertainty-aware tensor visualization in medical imaging. a) Comparison of two different tensor fields [ZSL*16]. b) Uncertainty-aware tensor glyphs with surrounding surfaces [GRT19].*

Zhang et al. [ZSL*16] provided a methodology to compare two different sets of tensors, as shown in Figure 17(a). They utilized *merged glyphs* to provide a visual representation for comparison. Although this allows solely the comparison of different datasets, one might be able to get a first impression of the variability in DTI datasets.

Gerrits et al. [GRT19] presented an uncertainty-aware visualization of tensor glyphs. In their methods, the tensor glyph is surrounded by a transparent hull that indicates the potential variation in the glyph appearance, as shown in Figure 17(b).

Abbasloo et al. [AWHS16] provided a visual analytics tool that allows a user to examine DTI datasets in an intuitive fashion. Starting from an uncertainty quantification, volume rendering, uncertainty-aware glyphs, and tractography are provided to allow clinicians to refine their diagnosis.

Ristovski et al. [RGH*19] used glyphs in a completely different manner. They aim to highlight areas in the brain that should be treated by radiofrequency to remove a tumor while not destroying surrounding tissue. The glyphs use a distinct color-coding to highlight the certainty of an area to be treated.

Summary: This section shows that visualization of uncertainty in medical imaging is hard to achieve as there does solely exist one approach (direct volume rendering= that is able to cover all the requirements that were defined.

5. Applications

In order to target a specific use case in medical imaging, medical imaging visualization pipelines need to be composed. In the following, we aim to summarize approaches of visualization for uncertainty-aware medical imaging that can be directly used in medical applications. Here, we structure the identified approaches along with four applications: diagnosis, treatment planning, intraoperative support, and education.

5.1. Diagnosis

Saad et al. [SMH10] devised an interactive segmentation algorithm where users can manipulate the aspects of the medical image that is visible to them. For diagnosis, this is a very important feature as the region of interest and the resulting segmentation target vary dramatically according to the underlying use case. The tool can be used to assist during diagnosis tasks where the shape and appearance of specific structures play an important role.

Unger et al. [UHP*20] presented a real-time diagnosis and visualization of tumor margins in excised breast specimens. They use Bayesian machine learning in order to determine tissue that is affected by a tumor. The probabilities are shown as color-coding in the original imaging data.

Gillmann et al. [GSW*20] developed a visual analysis tool that is able to examine the uncertainty of input CT scans, transforming this uncertainty throughout an uncertainty-aware image segmentation approach, indicating the resulting uncertainty in an indirect volume rendering approach to show which part of the brain might be affected by a lesion.

Brecheisen et al. [BPtHRV13] used illustrative volume rendering in order to capture a variety of potential tractographies obtained from a DTI scan, as shown in Figure 18(b). They embed the resulting visualization into a volume rendering of the brain to allow the examination of spatial variation in the captured tractography.

Ristovski et al. [RMW*17] presented an uncertainty-aware volume rendering method that allows users to directly see the potential dimension of stenotic regions in arteries. Here, several surfaces are shown to indicate different confidence intervals of the reviewed stenosis, as shown in Figure 18(a).

Gillmann et al. [GMHW18] provided an uncertainty-aware image-based indicator to early diagnose peripheral artery disease. They use an uncertainty-aware segmentation approach to compare a healthy and a diseased leg to locate differences between them.

5.2. Treatment Planning

A prominent application of medical imaging for treatment planning is the determination of dose radiation. Schlachter et al. [SRM*19] highlighted the importance of uncertainty-aware visualization in this application.

Wieser et al. [WCW*17] developed an open-source tool called matRad that allows the calculation of radiation at specific points in a patient's tissue. Their work computes the radiation dose using the underlying CT image and its uncertainty. The resulting visualization is a heatmap embedded in the original image data, as shown in Figure 18(c). This principle was refined by Maleike et al. [MUO06] considering probabilistic dose distributions, and Clements et al. [CST*18] allowing user input to define which areas should be aimed at with radiation. The tool then computes the potential radiation to the surrounding tissue.

Another important aspect of intraoperative support is the use of brain maps that aim to assign different regions to the human brain that map to the physical abilities of humans. These maps are often computed based on a sample of patients and it can be hard to determine the exact boundaries between different regions.

The Julich-Brain Atlas [AMBZ20] provides a brain atlas with fuzzy boundaries. The atlas is computed based on multiple patient

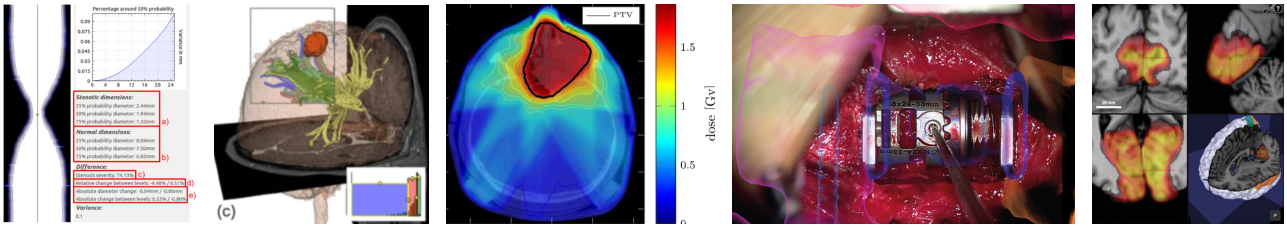

(a) (b) (c) (d) (e)

Figure 18: *Applications of uncertainty-aware visualization in medical imaging. a) Uncertainty-aware visualization of stenosis [RMW*17] using isosurfaces to indicate different stenosis stages. b) Illustrative rendering of tractographies [BPtHRV13] showing a summary of multiple paths surrounding a tumor. c) Uncertainty-aware visualization of radiation during therapy [WCW*17] indicating radiated tissue using color-coding. d) Uncertainty-aware guidance during surgery [CBS*19] using color and transparency to indicate potential missplacement of instruments. e) Uncertainty-aware brain atlas [AMBZ20] providing a color-coding that highlights uncertain areas.*

data and their degree of agreement is used to provide a probability for a specific voxel to be contained in a specific class of the brain, as shown in Figure 18(e). This atlas was used by Fox et al. [Fox18] who also included uncertainty-aware tractography computations that allow for examining the probability of a tractography to be located in a specific class of the brain atlas.

5.3. Intraoprative Support

A prominent example of intraoperative support is the use of medical imaging during surgeries or the planning process of surgeries.

Simpson et al. [SMC*06] provided guidance in surgery guidance by visually indicating the uncertainty of the registered surgery device during the surgery itself. The uncertainty is quantified by using *statistical analysis* which allows clinicians to identify the positional uncertainty of specific surgery tools.

Barbara et al. [CBS*19] presented a visual tool that indicates the positional uncertainty of tools used during surgery. The uncertainty was quantified using *trajectory alignment*. Their approach shows the potential distortion of the tools in visualizations, as shown in Figure 18(d).

Simpson et al. [SMV*14] computed and visualized the uncertainty throughout the use of surgical tools. They used a heat map to indicate the probability of a tool touching a specific tissue while considering the registration uncertainty during the registration process.

Gillmann et al. [GMP*18] provided an uncertainty-aware tool that allows planning minimally invasive surgeries. In their tool, the uncertainty of the input CT scans is captured while an uncertainty-aware segmentation approach is used to extract different types of tissues. This enables clinicians to define surgery paths and visualization is used to show the probability of interfering with different types of tissues.

5.4. Education

Although the positive effect of visualization approaches in medical education are well-known [FL18] and specific courses to teach image processing principles to medical students are designed [GWHH17], uncertainty is not covered in any of these works so far.

Summary: Considering applications, there exist approaches in each category that consider uncertainty except for education. Here, no approaches have been found.

6. Discussion

We showed that there exist a variety of uncertainty-aware visualization approaches in medical imaging and how these can be applied to different clinical scenarios. In this section, we aim to discuss whether the requirements that have been determined in section 3.3 are met by the presented approaches. Here, we made a ranking for all presented works. Our medical collaborators (3 clinicians) discussed our rating and corrected it if needed. In addition, we aim to provide a list that indicates which groups of medical imaging approaches can be combined in order to compose an entire image processing pipeline.

6.1. Check of Requirements

Table 2 shows all presented approaches for uncertainty-aware **Image Acquisition**. It can be seen that there exist solely two categories (Ultrasound and Computed Tomography) that hold uncertainty-aware medical imaging approaches. MRI, DTI, and PET approaches exist in an uncertainty-aware manner but do not fulfill all requirements.

Most presented approaches show the captured uncertainty in the input images using a separate image that provides a color-coding indicating the degree of uncertainty captured in an image voxel. This approach can be hard to correlate in clinical daily routine and is a clear violation of **R3**. Especially for DTI where multiple values per voxel need to be reviewed, an additional dimension of complexity may lead to cognitive overload. Here, we can clearly see that a direct correlation between the input image and its uncertainty in one intuitive view is an important aspect that needs more focus in this research area.

We have investigated a variety of uncertainty-aware **Image**

Acquisition	Work	R1	R2	R3
Ultrasound	[HCMC10]	✓	✗	✓
	[ZBDH*15]	✓	✓	✓
	[KWKN12]	✓	✓	✓
	[LBdJ18]	✗	✓	✓
	[GML14]	✗	✓	✓
Computed Tomography	[HLF14]	✗	✓	✓
	[TS16]	✗	✓	✓
	[RHH*20]	✗	✓	✓
	[GAH*17]	✓	✓	✓
Magnetic Resonance Imaging	[EMVP19]	✗	✓	✓
	[GDP*20]	✗	✓	✓
	[CVR19]	✓	✓	✗
Diffusion Tensor Imaging	[AMME18]	✗	✓	✓
	[WTW*08]	✗	✓	✓
	[BWJ*03]	✗	✓	✓
Positron Emission Imaging	[SSHM07]	✗	✓	✓
	[HBG*15]	✗	✓	✓
	[NBYR12]	✓	✓	✗

Table 2: *Check of uncertainty-aware **Image Acquisition** against the formulated requirements (**R1** Show the original dataset, **R2** Show the related uncertainty and **R3** Keep the cognitive load minimal). The approaches are sorted along with the subcategories of different acquisition techniques. Techniques that fulfill all requirements are highlighted in gray.*

Transformation approaches that we have sorted into several subcategories, as shown in Table 3. For image pre-processing, we were able to find approaches that fulfill all requirements for uncertainty-aware medical imaging visualization in both subcategories (image operations and image registration). For image operations we can see that most approaches do not aim to indicate the uncertainty visually. Instead, these approaches aim to use uncertainty information to enhance the image operation output.

For medical image segmentation, about a third of the approaches that we identified are able to fulfill all defined requirements. In this context, we want to highlight that Bayesian decision theory is a technique that becomes more popular in the field of visualization and potentially is a key element in fulfilling the formulated requirements.

In the category of feature extraction algorithms, the geometry extraction algorithms included in this report do not provide a method that allows for visualization of uncertainty-aware medical imaging that fulfills all defined requirements. This is probably due to the nature of surfaces and the relatively seldom use in clinical daily routine. On the other hand, all tractography-based visualization algorithms fulfill the defined requirements. This category impressively shows how original image and uncertainty information can be combined while providing an intuitive visualization for clinicians. Tractographies are embedded in a slice-by-slice view which makes it easy for clinicians to correlate the novel visualization technique with the well-known slice-by-slice reviewing technique.

Table 4 summarizes the identified techniques for the **visualization** step in medical imaging. The table indicates that there exists solely one approach that is able to fulfill the requirements for uncertainty-aware visualization in medical imaging. This approach uses direct volume rendering. The reason is that indirect volume rendering and glyph-based visualization are not used in all clinical settings. If it is used, structures that are rather clearly identified are shown such as bones or surface shaded displays in radiology stations. Therefore, the examined techniques are not able to present a visualization that meets the needs of clinicians in general. Here,

Transformation		Work	R1	R2	R3
Pre-Processing	Image Operations	[PAL01]	✓	✗	✗
		[MRSS08]	✓	✗	✗
		[JH01]	✓	✗	✗
		[LTAH13]	✓	✓	✗
		[FCC15]	✓	✗	✗
		[GPW*19]	✓	✓	✓
		[Cha15]	✓	✗	✗
	Image Registration	[LTAH13]	✗	✓	✓
		[BYW*20]	✗	✓	✓
		[LDCA17]	✗	✓	✓
		[RPSW10]	✓	✓	✓
		[YN15]	✓	✓	✓
		[SFJ*16]	✓	✓	✓
Segmentation		[BS09]	✓	✗	✗
		[CCZ07]	✓	✗	✗
		[AVvO*04]	✓	✗	✗
		[KT08]	✗	✓	✓
		[Ada12]	✗	✓	✓
		[HR18]	✓	✓	✓
		[LGM*14]	✗	✓	✓
		[ATHL14]	✗	✓	✓
		[SHM10]	✗	✓	✗
		[PRH10]	✓	✓	✓
		[BUK*10]	✗	✓	✓
		[ATHL15]	✓	✓	✗
		[GPW*19]	✗	✓	✓
		[KWKP20]	✓	✓	✓
		[NPAA20]	✓	✓	✓
Feature Extraction	Surface Extraction	[GMG09]	✓	✗	✗
		[DSS*09]	✓	✗	✗
		[PWH11]	✓	✗	✗
		[HMH*15]	✓	✓	✗
		[GWHA18]	✓	✓	✗
	Tracto-Graphy	[BBKW02]	✓	✓	✓
		[FFW06]	✓	✓	✓
		[CLH06]	✓	✓	✓
		[BBJ*07]	✓	✓	✓
		[BPVHR12]	✓	✓	✓

Table 3: *Check of uncertainty-aware **Image Transformation** against the formulated requirements (**R1** Show the original dataset, **R2** Show the related uncertainty and **R3** Keep the cognitive load minimal). The approaches are sorted along with the subcategories of different processing techniques. Techniques that fulfill all requirements are highlighted in gray.*

Visualization	Work	R1	R2	R3
Direct Volume Rendering	[Kni08]	✓	✓	✗
	[LLPY07]	✓	✓	✓
	[MCC*20]	✓	✓	✗
	[KSE16]	✓	✓	✓
Indirect Volume Rendering	[RLBS03]	✓	✓	✗
	[GR04]	✓	✓	✗
	[Dra08]	✓	✓	✗
	[GWHA18]	✓	✓	✗
Glyph-based Visualization	[Jon03]	✓	✓	✗
	[ZSL*16]	✓	✓	✗
	[GRT19]	✓	✓	✗
	[AWHS16]	✓	✓	✗
	[RGH*19]	✓	✓	✗

Table 4: *Check of uncertainty-aware **Image Visualization** against the formulated requirements (**R1** Show the original dataset, **R2** Show the related uncertainty and **R3** Keep the cognitive load minimal). The approaches are sorted along with the subcategories of different visualization techniques. Techniques that fulfill all requirements are highlighted in gray.*

a combination with the slice-by-slice reviewing approach is highly required in order to promote unused visualization approaches.

Application	Work	R1	R2	R3
Diagnosis	[SSHM07]	✓	✓	✗
	[GSW*20]	✗	✓	✓
	[BPtHRV13]	✓	✓	✓
	[RMW*17]	✗	✓	✓
	[GMHW18]	✓	✓	✓
Treatment Planning	[WCW*17]	✓	✓	✗
	[MUO06]	✗	✓	✓
	[CST*18]	✓	✓	✓
	[AMBZ20]	✗	✓	✗
	[Fox18]	✓	✓	✓
Intraoperative Support	[SMC*06]	✓	✓	✓
	[CBS*19]	✓	✓	✓
	[SMV*14]	✓	✓	✓
	[GMP*18]	✗	✓	✓
Education	-	-	-	-

Table 5: *Check of uncertainty-aware **Applications** against the formulated requirements (**R1** Show the original dataset, **R2** Show the related uncertainty and **R3** Keep the cognitive load minimal). The approaches are sorted along with the subcategories of different medical applications. Techniques that fulfill all requirements are highlighted in gray.*

Table 5 shows the examined approaches that are designed to target a specific **application** in uncertainty-aware medical imaging. Here, we directly see that we could not find any approaches that provide uncertainty-aware visualization in medical education, which might be due to the fact that medical students have to learn a lot. For the remaining categories, we were able to identify several approaches that assist in the respective task. In each category, there exist multiple approaches that fulfill the formulated requirements. In general, the table shows that approaches that are designed to aid in a specific task hold the highest potential in fulfilling all defined requirements. This indicates that medical imaging needs to be considered in its entirety instead of a single step. It also shows that combined properly, single image processing algorithms can form an uncertainty-aware medical imaging pipeline that provides a visualization that fulfills all defined requirements. For diagnosis, we found the highest variety of applications. They range from organ examination over tumor detection to the identification of stenotic regions. For treatment planning, we mostly identified tumor radiation approaches for uncertainty-aware visualization approaches. We postulate that more treatment applications could benefit from these techniques, such as ultrasound and ultraviolet therapies. Methods for intraoperative support could be found for surgery assistance mainly. This is due to the nature of this procedure, where medical images are used to follow the progress of surgery. Other applications for intraoperative support could be strengthened by medical imaging and uncertainty visualization as well if it gets used more frequently.

6.2. Creation of Medical Imaging Pipelines

As shown in section 4, there are plenty of techniques available for uncertainty-aware visualization in medical imaging. A summary of relevant work that we identified in this area can be found in Figure 19. Here, we included the three categories **Image Acquisition**, **Image Transformation** and **Image Visualization** with derived subcategories. In each category, we added the identified related work, which is described in section 4.

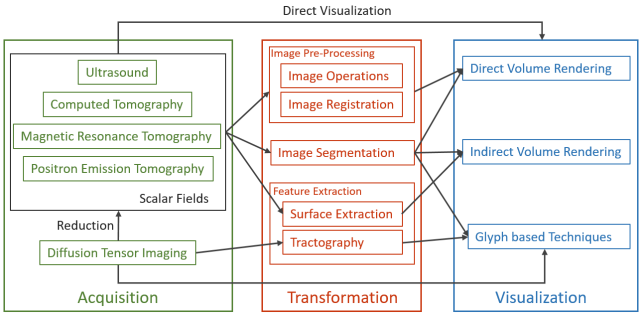

Figure 19: *Uncertainty-aware medical imaging and its subcategories examined as a pipeline. The arrows connect subcategories where output and input fit and can form a potential pipeline. If there is no connection indicated, no literature has been found that is able to connect these subcategories.*

Besides the reviewed application scenarios, we observed each category of medical imaging as an independent step and examined the available work in this area. But typically, medical imaging involves several steps. Our prior analysis showed that medical imaging needs to be considered as an entirety to be powerful. Technically, each step can be repeated multiple times thereby creating arbitrary medical imaging pipelines. In this section, we aim to declare the potential correlations between medical imaging steps in

the case that an output of an imaging step matches the input of another imaging step. In combination with the previously provided state-of-the-art analysis in each step, this provides a versatile way of forming arbitrary uncertainty-aware medical imaging pipelines.

Ultrasound images, Computed Tomography Images, Magnetic Resonance Tomography Images, and Positron Emission Imaging can be passed to image pre-processing segmentation algorithms and geometry extraction algorithms. As all this results in a dataset defined as a scalar field on a regular grid, image pre-processing algorithms are able to process these uncertainty-aware input images.

For diffusion tensor images, this does not hold as the previously mentioned operations are usually not able to process uncertainty-aware tensor fields. Still, Diffusion Tensor imaging might be able to be processed by image pre-processing, image segmentation, or surface extraction algorithms when simplifying the input image into scalar values. There are a variety of simplification metrics for tensors [VZKL06], but the incorporation of uncertainty does not work right away. Luckily, these methods can be extended to include the uncertainty information captured from the original DTI [BP00, And01, JB04, HAI*17].

Image pre-processing can be used as input for direct volume rendering. The resulting images from image operations, as well as image registration algorithms, create manipulated images that can be used as input for uncertainty-aware direct volume rendering. The same holds for image segmentation results. In addition, uncertainty-aware image segmentation results can be passed to surface extraction algorithms and therefore be passed to direct volume rendering. In general, uncertainty-aware image transformation outputs can be visualized utilizing indirect volume rendering approaches.

The described pathways can be directly used to create image processing pipelines and therefore allow for a flexible design of uncertainty-aware medical imaging.

6.3. The Curse of Uncertainty

Although we showed the importance of including uncertainty in the medical imaging process, uncertainty analysis can add multiple dimensions of uncertainty on top of each data point in the original dataset. Here, the question arises if and when it is feasible and worth taking the effort to include uncertainty into a medical imaging process.

This issue has been raised by Windhager et al. [WSSM19], in the domain of digital humanities. Hullman [Hul20] examined this issue generally in the visualization community. In his work, he researched reasons why uncertainty is often not included in visualization approaches. Hullman showed that most researchers aim to include uncertainty visualization, but are often overwhelmed by the possibilities of uncertainty visualization. As a result, uncertainty visualization is neglected in many cases.

These issues also occur in medical visualization and result in the problem to find a proper balance between visualizing uncertainty, while keeping the cognitive load in a visualization minimal. This is hard to determine, and further research in this direction is required.

7. Open Challenges

Although section 6 shows that uncertainty-aware medical imaging approaches can be found in most medical imaging steps and applications, there remains a set of open challenges, which will be discussed in the following.

7.1. Identification of proper Uncertainty Quantification Approaches

We have listed a variety of uncertainty quantification approaches that are suitable for medical imaging regarding specific cases and specific images or algorithms. Unfortunately, this prevents us from deriving a general rule for which uncertainty quantification applies best in each case. In each novel case or even if a case is only slightly different, uncertainty quantification algorithms need to be tested in order to determine their quality. This is a massive problem when dealing with uncertainty-aware medical imaging which remains an open problem.

7.2. Uncertainty in Clinical Studies

Uncertainty in clinical studies is not covered in this manuscript, as we aimed to provide a summary of uncertainty-aware visualization approaches. Still, this is an important issue as uncertainty in clinical studies holds two problems: first, assumptions for visualization approaches and the general applicability of image modalities are generated throughout these studies. Here, incorrect assumptions can lead to false conclusions when designing uncertainty-aware visualization. On the other hand, uncertainty-aware medical imaging approaches may be used to proceed with clinical studies. Therefore, the outcome of the clinical study is directly depending on the quality of the visualization.

7.3. Exploration Tools for Uncertainty in Medical Image Data

As shown in section 4.1, nearly all quantification approaches use color-coding to represent the resulting uncertainty quantification. This can lead to visual overload when adding this information to the input image or difficulty to understand the relationship between the input image and uncertainty quantification if using the color-coded uncertainty quantification next to the original image. In this case, there is a clear need to provide novel visualization approaches that help review both: the acquired image and the uncertainty quantification. This visualization should also include interaction methods that help users explore the uncertainty space in relation to the original dataset.

7.4. Knowledge from other Applications

Besides the medical domain, other application areas, such as mechanical engineering, deal with scalar and tensor fields [HBK*21]. These research areas are very active and the techniques developed in those areas could translate to the medical domain and provide novel insights into medical image data. Especially work that considers sensitivity analysis, multi-field visualization, and uncertainty in the acquisition step can be of great value for the presented topic. Still, the applicability of approaches other than the medical field needs to be proven in order for it to be suitable in the medical area.

7.5. Provenance Visualization of Uncertainty

As shown in section 6, medical imaging can be the starting point of an arbitrary pipeline. The uncertainty accumulates along this pipeline. Depending on the specific elements within this pipeline, the uncertainty of the dataset to be examined can dramatically increase. In this context, an understanding of how the uncertainty evolves throughout the application of multiple imaging steps would be beneficial. Here, provenance visualization techniques can be applied and more research is required to achieve this.

7.6. Teaching of uncertainty-aware Medical Imaging

Although section 3 shows that uncertainty plays a crucial role in medical imaging, these techniques are not well-known in the medical community. A major reason for this is the lack of education of uncertainty in medical imaging. Here, novel classes need to be established that help educate medical students to specialize in uncertainty analysis in a similar way as the general medical imaging class by Gillmann et al. [GWHH17].

7.7. Connection to Sensitivity and Ensemble Visualization

Besides uncertainty analysis itself, sensitivity analysis and ensemble analysis can be of great benefit to the medical imaging community. In fact, there is a strong relationship between all topics mentioned. For ensemble visualization [WHLS19], research that aims to summarize different data points in a visualization capturing the variation is of high interest for the given topic. Sensitivity analysis approaches that assist in understanding the impact of variations of parameters could be a great starting point for medical imaging as well. Here, methodologies from sensitivity and ensemble analysis should be considered for their potential applicability in medical imaging.

7.8. Further use of Machine Learning

As shown in section 4, machine learning is a popular tool for uncertainty-aware medical algorithms across all imaging steps. This set of methods is of great interest as it provides promising results in a variety of medical imaging tasks. We believe that the use of machine learning could improve the field of medical visualization dramatically. Still, there are a variety of downsides when using machine learning approaches (especially neural networks). The most important is that neural networks form a black box. Here, users are not able to directly follow the computation of the neural network. This is especially critical in the medical area as medical doctors are responsible for their decisions and therefore need a way to verify the computational result of an algorithm. Ongoing work with respect to explainability for machine learning may eventually resolve this issue.

7.9. Visual Analytics Approaches in Medical Imaging

In medical imaging, often multiple steps of the computational pipeline need to be considered to provide a holistic analysis of patient data. In addition, machine learning approaches become increasingly important. Depending on the medical tasks (diagnosis, surgery planning, etc.) different medical image steps need to be combined and clinicians need to be enabled to examine and interact with these techniques. Here, visual analytics approaches can be a suitable approach. Visual analytics describes a holistic visual approach where data can be processed by hypothesis forming and using visualizations to create novel knowledge [KMS*08]. Sacha et al. [SSK*16] highlighted the importance of proper communication of uncertainty in the visual analytics process.

There exist first attempts to provide visual analytics approaches in medical imaging, such as Gillmann et al. [GMHW18] that aim to assist in minimally invasive planning or Brecheisen et al. [BVPt09] providing a visual analytics tool that allows the user to visually explore how small variations in parameter values affect the output of fiber tracking. However, these methods are still in their infancy. In addition, the concepts of visual analytics are not fully incorporated in the listed research papers. We suggest a more holistic use of visual analytics approach in the area of medical imaging.

7.10. Ready to use Framework

As shown in section 6, a variety of potential uncertainty-aware imaging pipelines can be created while communicating uncertainty [GWH16, MSH*20]. Still, the question arises as to which of these pipelines really provide insight for clinicians. Further, it is unclear which use cases can be covered by which pipeline. We, therefore, encourage the development of a flexible and easy to adjust framework for uncertainty-aware medical imaging to allow easy and fast testing.

7.11. Clinical Trials on Uncertainty-aware Medical Imaging

To the best of our knowledge, there does not exist any commercially available visualization technique in medical workstations that is uncertainty-aware. This may indicate that uncertainty visualization research is driven by visualization researchers rather than clinicians. Here, we suggest defining selected diagnostic decisions where the hypothesis is that uncertainty visualization is beneficial. This hypothesis should then be confirmed or rejected in close collaboration with physicians. This can be achieved by a clinical study where perception, cognition, and interpretation with respect to uncertainty visualization can be examined.

8. Conclusions

In this manuscript, we provide a state-of-the-art analysis of uncertainty-aware medical imaging. We provide an overview of medical imaging in general and determined the special role of uncertainty in this area. Resulting from that, we compiled a taxonomy of uncertainties in medical imaging and defined requirements that need to be fulfilled to provide a suitable visualization. Our state-of-the-art analysis is structured along the medical imaging pipeline consisting of Image Acquisition, Image Transformation, and Image Visualization. We further examined uncertainty-aware visualization approaches in applications of medical imaging. Based on the defined requirements, we outlined the suitability of the examined approaches in the given context. Furthermore, we provided a list of open problems that have not been tackled in the area of medical imaging.

References

[Ada12] ADAMS R. P.: Revisiting uncertainty in graph cut solutions. In *Proceedings of the 2012 IEEE Conference on Computer Vision and Pattern Recognition (CVPR)* (2012), IEEE Computer Society, pp. 2440–2447. 11, 17

[AMBZ20] AMUNTS K., MOHLBERG H., BLUDAU S., ZILLES K.: Julich-brain: A 3d probabilistic atlas of the human brain's cytoarchitecture. *Science 369*, 6506 (2020), 988–992. 15, 16, 18

[AMME18] ALIOTTA E., MOULIN K., MAGRATH P., ENNIS D. B.: Quantifying precision in cardiac diffusion tensor imaging with second-order motion-compensated convex optimized diffusion encoding. *Magnetic Resonance in Medicine 80*, 3 (2018), 1074–1087. 9, 17

[And01] ANDERSON A. W.: Theoretical analysis of the effects of noise on diffusion tensor imaging. *Magnetic Resonance in Medicine 46*, 6 (2001), 1174–1188. 19

[ASV*18] ALAM I., STEINBERG I., VERMESH O., VAN DEN BERG N., ROSENTHAL E., VAN DAM G., NTZIACHRISTOS V., GAMBHIR S., HERNOT S., ROGALLA S.: Emerging intraoperative imaging modalities to improve surgical precision. *Mol. Imaging Biol. 20*, 5 (2018), 705–715. 5

[ATHL14] AL-TAIE A., HAHN H. K., LINSEN L.: Uncertainty estimation and visualization in probabilistic segmentation. *Computers & Graphics 39* (2014), 48 – 59. 11, 12, 17

[ATHL15] AL-TAIE A., HAHN H. K., LINSEN L.: Uncertainty Estimation and Visualization for Multi-modal Image Segmentation. In *Eurographics Workshop on Visual Computing for Biology and Medicine* (2015), The Eurographics Association. 11, 17

[AU19] ATABO S. M., UMAR A.: A review of imaging techniques in scientific research/clinical diagnosis. *MOJ Anatomy & Physiology 6* (10 2019). 3

[AVvO*04] ANBEEK P., VINCKEN K. L., VAN OSCH M. J., BISSCHOPS R. H., VAN DER GROND J.: Probabilistic segmentation of white matter lesions in mr imaging. *NeuroImage 21*, 3 (2004), 1037 – 1044. 11, 17

[AWHS16] ABBASLOO A., WIENS V., HERMANN M., SCHULTZ T.: Visualizing tensor normal distributions at multiple levels of detail. *IEEE Transactions on Visualization and Computer Graphics 22*, 1 (2016), 975–984. 15, 18

[BAL12] BRODLIE K., ALLENDES OSORIO R., LOPES A.: *A Review of Uncertainty in Data Visualization*. Springer London, London, 2012, pp. 81–109. 2

[Ban08] BANKMAN I.: *Handbook of medical image processing and analysis*. Elsevier, 2008. 4

[BBC87] BELFORTE G., BONA B., CERONE V.: Bounded measurement error estimates: Their properties and their use for small sets of data. *Measurement 5*, 4 (1987), 167 – 175. 5

[BBJ*07] BEHRENS T., BERG H. J., JBABDI S., RUSHWORTH M., WOOLRICH M.: Probabilistic diffusion tractography with multiple fibre orientations: What can we gain? *NeuroImage 34*, 1 (2007), 144 – 155. 13, 17

[BBKW02] BJÖRNEMO M., BRUN A., KIKINIS R., WESTIN C.-F.: Regularized stochastic white matter tractography using diffusion tensor mri. In *Medical Image Computing and Computer-Assisted Intervention — MICCAI 2002* (Berlin, Heidelberg, 2002), Springer Berlin Heidelberg, pp. 435–442. 13, 17

[BHJ*14] BONNEAU G.-P., HEGE H.-C., JOHNSON C. R., OLIVEIRA M. M., POTTER K., RHEINGANS P., SCHULTZ T.: *Overview and State-of-the-Art of Uncertainty Visualization*. Springer London, 2014, pp. 3–27. 2

[BHP15] BOUMANS M., HON G., PETERSEN A. C.: *Error and uncertainty in scientific practice*. Routledge, 2015. 5

[BJ15] BOYAT A. K., JOSHI B. K.: A review paper: Noise models in digital image processing. *CoRR abs/1505.03489* (2015). 5

[BKC*13] BORGO R., KEHRER J., CHUNG D., MAGUIRE E., LARAMEE R., HAUSER H., WARD M., CHEN M.: Glyph-based visualization: Foundations, design guidelines, techniques and applications. In *Eurographics (STARs)* (05 2013), pp. 39–63. 4

[BP00] BASSER P. J., PAJEVIC S.: Statistical artifacts in diffusion tensor mri (dt-mri) caused by background noise. *Magnetic Resonance in Medicine 44*, 1 (2000), 41–50. 19

[BPtHRV13] BRECHEISEN R., PLATEL B., TER HAAR ROMENY B., VILANOVA A.: Illustrative uncertainty visualization of dti fiber pathways. *The Visual Computer 29* (04 2013). 15, 16, 18

[BPVHR12] BRECHEISEN R., PLATEL B., VILANOVA A., HAAR ROMENY B. T.: Illustrative uncertainty visualization of dti fiber pathways. *The Visual Computer* (2012). 13, 17

[Bra08] BRADLEY W. G.: History of medical imaging. *Proceedings of the American Philosophical Society 152*, 3 (2008), 349–361. 1

[Bru17] BRUNO M. A.: 256 shades of gray: uncertainty and diagnostic error in radiology. *Diagnosis 4*, 3 (2017), 149 – 157. 1

[BS09] BEEVI Z., SATHIK M.: A robust segmentation approach for noisy medical images using fuzzy clustering with spatial probability. *International Arab Journal of Information Technology 29*, 37 (2009), 38. 11, 17

[BUK*10] BATRA D., UNIVERITY C. M., KOWDLE A., PARIKH D., LUO J., CHEN T.: icoseg: Interactive co-segmentation with intelligent scribble guidance. In *In CVPR* (2010). 11, 12, 17

[Bur11] BURGESS A.: Visual perception studies and observer models in medical imaging. *Seminars in nuclear medicine 41* (11 2011), 419–36. 4

[BVPt09] BRECHEISEN R., VILANOVA A., PLATEL B., TER HAAR ROMENY B.: Parameter sensitivity visualization for dti fiber tracking. *IEEE Transactions on Visualization and Computer Graphics 15*, 6 (2009), 1441–1448. 20

[BWJ*03] BEHRENS T., WOOLRICH M., JENKINSON M., JOHANSEN-BERG H., NUNES R., CLARE S., MATTHEWS P., BRADY J., SMITH S.: Characterization and propagation of uncertainty in diffusion-weighted mr imaging. *Magnetic Resonance in Medicine 50*, 5 (2003), 1077–1088. 9, 17

[BYW*20] BIAN C., YUAN C., WANG J., LI M., YANG X., YU S., MA K., YUAN J., ZHENG Y.: Uncertainty-aware domain alignment for anatomical structure segmentation. *Medical Image Analysis 64* (2020). 10, 17

[BZK03] BASIR O., ZHU H., KARRAY F.: Fuzzy based image segmentation. In *Fuzzy Filters for Image Processing*. Springer, 2003, pp. 101–128. 4

[Cat03] CATTANEO M.: Combining belief functions issued from dependent sources. In *Research report/Seminar für Statistik, Eidgenössische Technische Hochschule (ETH)* (01 2003), pp. 133–147. 6

[CBS*19] CARL B., BOPP M., SASS B., POJSKIC M., GJORGJEVSKI M., VOELLGER B., NIMSKY C.: Reliable navigation registration in cranial and spine surgery based on intraoperative computed tomography. *Neurosurgical Focus FOC 47*, 6 (2019). 16, 18

[CCZ07] CAI W., CHEN S., ZHANG D.: Fast and robust fuzzy c-means clustering algorithms incorporating local information for image segmentation. *Pattern Recogn. 40*, 3 (Mar. 2007), 825–838. 11, 17

[CFJ*06] COROUGE I., FLETCHER P. T., JOSHI S., GOUTTARD S., GERIG G.: Fiber tract-oriented statistics for quantitative diffusion tensor mri analysis. *Medical Image Analysis 10*, 5 (2006), 786 – 798. The Eighth International Conference on Medical Imaging and Computer Assisted Intervention – MICCAI 2005. 13

[Cha15] CHAIRA T.: *Medical Image Processing - advanced fuzzy set theoretic techniques*. CRC Press, 01 2015. 10, 17

[Che09] CHEN W.: A comparative study of uncertainty propagation methods for black-box-type problems. *Structural and Multidisciplinary Optimization 37* (01 2009), 239–253. 10

[CLH06] CHUNG S., LU Y., HENRY R. G.: Comparison of bootstrap approaches for estimation of uncertainties of dti parameters. *NeuroImage 33*, 2 (2006), 531 – 541. 13, 17

[CLP18] CHINMAYI P., LOGANATHAN A., PRABUKUMAR M.: Survey of image processing techniques in medical image analysis: Challenges and methodologies. In *International Conference on Soft Computing and Pattern Recognition* (12 2018), Advances in Intelligent Systems and Computing, pp. 460–471. 4

[Coo01] COOTNEY R. W.: Ultrasound Imaging: Principles and Applications in Rodent Research. *ILAR Journal 42*, 3 (07 2001), 233–247. 3

[CST*18] CLEMENTS M., SCHUPP N., TATTERSALL M., BROWN A., LARSON R.: Monaco treatment planning system tools and optimization processes. *Medical Dosimetry 43*, 2 (2018), 106 – 117. Special Issue: 3D Treatment Planning Systems. 15, 18

[CVR19] CROCI M., VINJE V., ROGNES M. E.: Uncertainty quantification of parenchymal tracer distribution using random diffusion and convective velocity fields. *bioRxiv* (2019). 9, 17

[DDKA09] DESCOTEAUX M., DERICHE R., KNOSCHE T. R., ANWANDER A.: Deterministic and probabilistic tractography based on complex fibre orientation distributions. *IEEE Transactions on Medical Imaging 28*, 2 (2009), 269–286. 13

[Dra08] DRAPIKOWSKI P.: Surface modeling—uncertainty estimation and visualization. *Computerized Medical Imaging and Graphics 32*, 2 (2008), 134 – 139. 14, 18

[DSS*09] DIETRICH C. A., SCHEIDEGGER C. E., SCHREINER J., COMBA J. L. D., NEDEL L. P., SILVA C. T.: Edge transformations for improving mesh quality of marching cubes. *IEEE Transactions on Visualization and Computer Graphics 15*, 1 (2009), 150–159. 12, 17

[EMVP19] EDUPUGANTI V., MARDANI M., VASANAWALA S., PAULY J.: Uncertainty quantification in deep mri reconstruction, 2019. 9, 17

[FCC15] FRANCO A., CORREIA M., CRUZ J.: Uncertainty propagation in biomedical models. In *Artificial Intelligence in Medicine* (Cham, 2015), Springer International Publishing, pp. 166–171. 10, 17

[FFW06] FRIMAN O., FARNEBACK G., WESTIN C. .: A bayesian approach for stochastic white matter tractography. *IEEE Transactions on Medical Imaging 25*, 8 (2006), 965–978. 13, 17

[FL18] FIRAT E. E., LARAMEE R. S.: Towards a survey of interactive visualization for education. *EG UK Computer Graphics & Visual Computing* (2018). 16

[Fox18] FOX M.: Mapping symptoms to brain networks with the human connectome. *New England Journal of Medicine 379* (12 2018), 2237–2245. 16, 18

[FP17] FERRANTE E., PARAGIOS N.: Slice-to-volume medical image registration: A survey. *Medical Image Analysis 39* (2017), 101–123. 7

[GAH*17] GILLMANN C., ARBELÁEZ P., HERNÁNDEZ J. T., HAGEN H., WISCHGOLL T.: Intuitive Error Space Exploration of Medical Image Data in Clinical Daily Routine. In *EG/VGTC Conference on Visualization (EuroVis) - Short Papers* (2017). 8, 17

[GAH*18] GILLMANN C., ARBELAEZ P., HERNANDEZ J. T., HAGEN H., WISCHGOLL T.: An uncertainty-aware visual system for image preprocessing. *Journal of Imaging 4*, 9 (2018). 10

[GDP*20] GLANG F., DESHMANE A., PROKUDIN S., MARTIN F., HERZ K., LINDIG T., BENDER B., SCHEFFLER K., ZAISS M.: Deepcest 3t: Robust mri parameter determination and uncertainty quantification with neural networks—application to cest imaging of the human brain at 3t. *Magnetic Resonance in Medicine 84*, 1 (2020), 450–466. 8, 9, 17

[GMG09] GLANZNIG M., MALIK M. M., GRÖLLER M. E.: Locally adaptive marching cubes through iso-value variation. In *Proceedings of the International Conference in Central Europe on Computer Graphics, Visualization and Computer Vision* (2009), pp. 33–40. 12, 13, 17

[GMHW18] GILLMANN C., MATSUURA J. H., HAGEN H., WISCHGOLL T.: Towards an Image-based Indicator for Peripheral Artery Disease Classification and Localization. In *Leipzig Symposium on Visualization In Applications* (2018). 15, 18, 20

[GML14] GUEZIRI H.-E., MCGUFFIN M., LAPORTE C.: Visualizing positional uncertainty in freehand 3d ultrasound. *Proceedings - Society of Photo-Optical Instrumentation Engineers 9036* (03 2014). 8, 17

[GMP*18] GILLMANN C., MAACK R. G. C., POST T., WISCHGOLL T., HAGEN H.: An uncertainty-aware workflow for keyhole surgery planning using hierarchical image semantics. *Visual Informatics 2*, 1 (2018), 26 – 36. Proceedings of PacificVAST 2018. 16, 18

[GPW*19] GILLMANN C., POST T., WISCHGOLL T., HAGEN H., MACIEJEWSKI R.: Hierarchical image semantics using probabilistic path propagations for biomedical research. *IEEE Computer Graphics and Applications* (2019), 1–1. 12, 17

[GR04] GRIGORYAN G., RHEINGANS P.: Point-based probabilistic surfaces to show surface uncertainty. *IEEE Transactions on Visualization and Computer Graphics 10*, 5 (2004), 564–573. 14, 18

[GRT19] GERRITS T., RÖSSL C., THEISEL H.: Towards glyphs for uncertain symmetric second-order tensors. *Computer Graphics Forum 38*, 3 (2019), 325–336. 14, 15, 18

[GSW*20] GILLMANN C., SAUR D., WISCHGOLL T., HOFFMANN K.-T., HAGEN H., MACIEJEWSKI R., SCHEUERMANN G.: Uncertainty-aware Brain Lesion Visualization. In *Eurographics Workshop on Visual Computing for Biology and Medicine* (2020), The Eurographics Association. 15, 18

[GWH16] GILLMANN C., WISCHGOLL T., HAGEN H.: Uncertainty-Awareness in Open Source Visualization Solutions. In *IEEE Visualization Conference (VIS) - VIP Workshop* (2016). 20

[GWHA18] GILLMANN C., WISCHGOLL T., HAMANN B., AHRENS J.: Modeling and visualization of uncertainty-aware geometry using multivariate normal distributions. In *2018 IEEE Pacific Visualization Symposium (PacificVis)* (April 2018), pp. 106–110. 14, 17, 18

[GWHH17] GILLMANN C., WISCHGOLL T., HERNÁNDEZ J. T., HAGEN H.: Teaching image processing and visualization principles to medicine students. *IEEE Visualization Conference (VIS) - Pedagogy of Data Visualization Workshop* (2017). 16, 20

[GWHH18] GILLMANN C., WISCHGOLL T., HAMANN B., HAGEN H.: Accurate and reliable extraction of surfaces from image data using a multi-dimensional uncertainty model. *Graphical Models 99* (2018), 13 – 21. 13

[HAI*17] HUTCHINSON E. B., AVRAM A. V., IRFANOGLU M. O., KOAY C. G., BARNETT A. S., KOMLOSH M. E., ÖZARSLAN E., SCHWERIN S. C., JULIANO S. L., PIERPAOLI C.: Analysis of the effects of noise, dwi sampling, and value of assumed parameters in diffusion mri models. *Magnetic Resonance in Medicine 78*, 5 (2017), 1767–1780. 19

[HB97] HASHEMI R., BRADLEY W. G.: *MRI: The Basics*. Williams & Wilkins, 1997. 4

[HBG*15] HUET P., BURG S., GULUDEC D., HYAFIL F., BUVAT I.: Variability and uncertainty of 18f-fdg pet imaging protocols for assessing inflammation in atherosclerosis: Suggestions for improvement. *Journal of nuclear medicine : official publication, Society of Nuclear Medicine 56* (02 2015). 9, 17

[HBK*21] HERGL C., BLECHA C., KRETZSCHMAR V., RAITH F., GÜNTHER F., STOMMEL M., JANKOWAI J., HOTZ I., NAGEL T., SCHEUERMANN G.: Visualization of tensor fields in mechanics. *Computer Graphics Forum* (2021). 19

[HCMC10] HELLIER P., COUPÉ P., MORANDI X., COLLINS D. L.: An automatic geometrical and statistical method to detect acoustic shadows in intraoperative ultrasound brain images. *Medical Image Analysis 14*, 2 (2010), 195 – 204. 8, 17

[HDF10] HASINOFF S. W., DURAND F., FREEMAN W. T.: Noise-optimal capture for high dynamic range photography. In *2010 IEEE*

Computer Society Conference on Computer Vision and Pattern Recognition (June 2010), pp. 553–560. 5

[Hel08] HELTON J. C.: Uncertainty and sensitivity analysis for models of complex systems. In *Computational Methods in Transport: Verification and Validation* (Berlin, Heidelberg, 2008), Springer Berlin Heidelberg, pp. 207–228. 5

[HFPN90] HÖHNE K., FUCHS H., PIZER S., NORTH ATLANTIC TREATY ORGANIZATION. SCIENTIFIC AFFAIRS DIVISION: *3D Imaging in Medicine: Algorithms, Systems, Applications*. NATO ASI Series : Advanced Science Institutes Series: Series F, Computer and system sciences. Springer-Verlag, 1990. 4

[HFSR19] HARMS R., FRITZ F., SCHOENMAKERS S., ROEBROECK A.: Fast quantification of uncertainty in non-linear diffusion mri models for artifact detection and more power in group studies. *bioRxiv* (2019). 8, 9

[HLF14] HOWARD M., LUTTMAN A., FOWLER M.: Sampling-based uncertainty quantification in deconvolution of x-ray radiographs. *Journal of Computational and Applied Mathematics 270* (2014), 43 – 51. Fourth International Conference on Finite Element Methods in Engineering and Sciences (FEMTEC 2013). 8, 17

[HMH*15] HE Y., MIRZARGAR M., HUDSON S., KIRBY R. M., WHITAKER R. T.: An uncertainty visualization technique using possibility theory: Possibilistic marching cubes. *International Journal for Uncertainty Quantification 5*, 5 (2015), 433–451. 13, 17

[HQC*19] HULLMAN J., QIAO X., CORRELL M., KALE A., KAY M.: In pursuit of error: A survey of uncertainty visualization evaluation. *IEEE Transactions on Visualization and Computer Graphics 25*, 1 (Jan 2019), 903–913. 2

[HR18] HERSHKOVITCH T., RIKLIN-RAVIV T.: Model-dependent uncertainty estimation of medical image segmentation. In *2018 IEEE 15th International Symposium on Biomedical Imaging (ISBI 2018)* (2018), pp. 1373–1376. 11, 17

[HSM08] HUETTEL S., SONG A., MCCARTHY G.: *Functional Magnetic Resonance Imaging, Second Edition*. Palgrave Macmillan, 12 2008. 9

[Hul20] HULLMAN J.: Why authors don't visualize uncertainty. *IEEE Transactions on Visualization & Computer Graphics 26*, 01 (jan 2020), 130–139. 19

[JA19] JENA R., AWATE S. P.: A bayesian neural net to segment images with uncertainty estimates and good calibration. In *Information Processing in Medical Imaging* (Cham, 2019), Springer International Publishing, pp. 3–15. 12

[JB04] JONES D. K., BASSER P. J.: "squashing peanuts and smashing pumpkins": How noise distorts diffusion-weighted mr data. *Magnetic Resonance in Medicine 52*, 5 (2004), 979–993. 19

[JED*20] JENA A., ENGELKE U., DWYER T., RAIAMANICKAM V., PARIS C.: Uncertainty visualisation: An interactive visual survey. In *2020 IEEE Pacific Visualization Symposium (PacificVis)* (2020), pp. 201–205. 2

[JH01] JI Q., HARALICK R. M.: Error propagation for the hough transform. *Pattern Recognition Letters 22*, 6 (2001), 813 – 823. 10, 17

[Jon03] JONES D. K.: Determining and visualizing uncertainty in estimates of fiber orientation from diffusion tensor mri. *Magnetic Resonance in Medicine 49*, 1 (2003), 7–12. 14, 18

[Jon08] JONES D. K.: Tractography gone wild: Probabilistic fibre tracking using the wild bootstrap with diffusion tensor mri. *IEEE Transactions on Medical Imaging 27*, 9 (2008), 1268–1274. 13

[Jä08] JÄHNE B.: *Digital image processing*. Prentice Hall, 2008. 4

[KAS97] KALET I. J., AUSTIN-SEYMOUR M. M.: The Use of Medical Images in Planning and Delivery of Radiation Therapy. *Journal of the American Medical Informatics Association 4*, 5 (09 1997), 327–339. 4

[KMM*18] KREISER J., MEUSCHKE M., MISTELBAUER G., PREIM B., ROPINSKI T.: A survey of flattening-based medical visualization techniques. *Computer Graphics Forum 37* (06 2018), 597–624. 2

[KMS*08] KEIM D. A., MANSMANN F., SCHNEIDEWIND J., THOMAS J., ZIEGLER H.: Visual analytics: Scope and challenges. In *Visual Data Mining*, vol. 4404 of *Lecture Notes in Computer Science*. Springer, 2008, pp. 76–90. 20

[Kni08] KNISS J.: Managing uncertainty in visualization and analysis of medical data. *IEEE International Symposium on Biomedical Imaging* (06 2008), 832 – 835. 14, 18

[KSE16] KROES T., SCHUT D., EISEMANN E.: Smooth probabilistic ambient occlusion for volume rendering. In *GPU Pro 6*. CRC Press, 2016, pp. 475–485. 14, 18

[KT08] KOHLI P., TORR P. H. S.: Measuring uncertainty in graph cut solutions. *Comput. Vis. Image Underst. 112*, 1 (2008), 30–38. 11, 17

[KWKN12] KARAMALIS A., WEIN W., KLEIN T., NAVAB N.: Ultrasound confidence maps using random walks. *Medical image analysis 16* (08 2012), 1101–12. 8, 17

[KWKP20] KWON Y., WON J.-H., KIM B. J., PAIK M. C.: Uncertainty quantification using bayesian neural networks in classification: Application to biomedical image segmentation. *Computational Statistics & Data Analysis 142* (2020). 12, 17

[LBdJ18] LULICH S. M., BERKSON K. H., [DE JONG] K.: Acquiring and visualizing 3d/4d ultrasound recordings of tongue motion. *Journal of Phonetics 71* (2018), 410 – 424. 8, 17

[LBMP*01] LE BIHAN D., MANGIN J.-F., POUPON C., CLARK C. A., PAPPATA S., MOLKO N., CHABRIAT H.: Diffusion tensor imaging: Concepts and applications. *Journal of Magnetic Resonance Imaging 13*, 4 (2001), 534–546. 4

[LC87] LORENSEN W. E., CLINE H. E.: Marching cubes: A high resolution 3d surface construction algorithm. In *Proceedings of the 14th Annual Conference on Computer Graphics and Interactive Techniques* (1987), SIGGRAPH '87, ACM, pp. 163–169. 12

[LDCA17] LE FOLGOC L., DELINGETTE H., CRIMINISI A., AYACHE N.: Quantifying registration uncertainty with sparse bayesian modelling. *IEEE Transactions on Medical Imaging 36*, 2 (2017), 607–617. 10, 11, 17

[LEE12] LIN G., ENGEL D. W., ESLINGER P. W.: *Survey and Evaluate Uncertainty Quantification Methodologies*. Tech. rep., Pacific Northwest National Lab.(PNNL), Richland, WA (United States), 2012. 5

[LFM*15] LIGUORI C., FRAUENFELDER G., MASSARONI C., SACCOMANDI P., GIURAZZA F., PITOCCO F., MARANO R., SCHENA E.: Emerging clinical applications of computed tomography. *Medical Devices: Evidence and Research 8* (06 2015), 265–78. 3

[LGM*14] LELANDAIS B., GARDIN I., MOUCHARD L., VERA P., RUAN S.: Dealing with uncertainty and imprecision in image segmentation using belief function theory. *Int. J. Approx. Reasoning 55*, 1 (2014), 376–387. 11, 17

[LLPY07] LUNDSTRÖM C., LJUNG P., PERSSON A., YNNERMAN A.: Uncertainty visualization in medical volume rendering using probabilistic animation. *Visualization and Computer Graphics, IEEE Transactions on 13* (12 2007), 1648 – 1655. 14, 18

[LML*07] LIU J., MA W., LIU F., HU Y., YANG J., XU X.: Study and application of medical image visualization technology. In *Digital Human Modeling* (Berlin, Heidelberg, 2007), Springer Berlin Heidelberg, pp. 668–677. 4

[LSBP17] LAWONN K., SMIT N., BÜHLER K., PREIM B.: A survey on multimodal medical data visualization. *Computer Graphics Forum 37* (10 2017). 2

[LTAH13] LOTFI T., TANG L., ANDREWS S., HAMARNEH G.: Improving probabilistic image registration via reinforcement learning and uncertainty evaluation. In *International Workshop on Machine Learning in Medical Imaging* (01 2013), pp. 188–195. 10, 17

[LvB17] LOUCKS D. P., VAN BEEK E.: *An Introduction to Probability, Statistics, and Uncertainty*. Springer International Publishing, Cham, 2017, pp. 213–300. 5

[LWA*20] LEVONTIN P., WALTON J., AUFEGGER L., BARONS M., BARONS E., FRENCH S., HOUSSINEAU J., KLEINEBERG J., MCBRIDE M., SMITH J.: *Visualising Uncertainty: A short introduction*. Sad Press, 01 2020. 1

[MA19] MEHTA R., ARBEL T.: 3d u-net for brain tumour segmentation. In *Brainlesion: Glioma, Multiple Sclerosis, Stroke and Traumatic Brain Injuries* (Cham, 2019), Springer International Publishing, pp. 254–266. 12

[MCC*20] MA J., CHEN J., CHEN L., JIN L., QIN X.: Dynamic visualization of uncertainties in medical feature of interest. *IEEE Access 8* (2020), 119170–119183. 14, 18

[Mor07] MORI S.: Chapter 9 - three-dimensional tract reconstruction. In *Introduction to Diffusion Tensor Imaging*. Elsevier Science B.V., Amsterdam, 2007, pp. 93 – 123. 13

[MPG*16] MIRAMS G. R., PATHMANATHAN P., GRAY R. A., CHALLENOR P., CLAYTON R. H.: Uncertainty and variability in computational and mathematical models of cardiac physiology. *The Journal of Physiology 594*, 23 (2016), 6833–6847. 7

[MRSS08] MENCATTINI A., RABOTTINO G., SALICONE S., SALMERI M.: Uncertainty handling and propagation in x-ray images analysis systems by means of random-fuzzy variables. In *2008 IEEE International Workshop on Advanced Methods for Uncertainty Estimation in Measurement* (July 2008), pp. 50–55. 10, 17

[MSH*20] MAACK R. G. C., SAUR D., HAGEN H., SCHEUERMANN G., GILLMAN C.: Towards closing the gap of medical visualization research and clinical daily routine. In *VisGap - The Gap between Visualization Research and Visualization Software* (2020), The Eurographics Association. 7, 20

[MUO06] MALEIKE D., UNKELBACH J., OELFKE U.: Simulation and visualization of dose uncertainties due to interfractional organ motion. *Physics in medicine and biology 51* (06 2006), 2237–52. 15, 18

[NBYR12] NGUYEN K. T., BOCK A., YNNERMAN A., ROPINSKI T.: Deriving and Visualizing Uncertainty in Kinetic PET Modeling. In *Eurographics Workshop on Visual Computing for Biology and Medicine* (2012), The Eurographics Association. 9, 17

[NMI10] NAZ S., MAJEED H., IRSHAD H.: Image segmentation using fuzzy clustering: A survey. In *Emerging Technologies (ICET), 2010 6th International Conference on* (Oct 2010), pp. 181–186. 11

[NPAA20] NAIR T., PRECUP D., ARNOLD D. L., ARBEL T.: Exploring uncertainty measures in deep networks for multiple sclerosis lesion detection and segmentation. *Medical Image Analysis 59* (2020). 12, 17

[Nud86] NUDELMAN S.: Image acquisition devices and their application to diagnostic medicine. In *Pictorial Information Systems in Medicine* (Berlin, Heidelberg, 1986), Springer Berlin Heidelberg, pp. 29–104. 3

[OM02] OLSTON C., MACKINLAY J. D.: Visualizing data with bounded uncertainty. In *Proceedings of the IEEE Symposium on Information Visualization (InfoVis'02)* (USA, 2002), INFOVIS '02, IEEE Computer Society, p. 37. 2, 5

[PAL01] PAL S. K.: Fuzzy image processing and recognition: Uncertainty handling and applications. *International Journal of Image and Graphics 01*, 02 (2001), 169–195. 10, 17

[PB07] PREIM B., BARTZ D.: *Visualization in Medicine: Theory, Algorithms, and Applications*. Morgan Kaufmann Publishers Inc., San Francisco, CA, USA, 2007. 1, 3, 7

[PB14a] PREIM B., BOTHA C.: Chapter 1 - introduction. In *Visual Computing for Medicine (Second Edition)*, second edition ed. Morgan Kaufmann, Boston, 2014, pp. 1 – 11. 1, 3

[PB14b] PREIM B., BOTHA C.: Chapter 6 - surface rendering. In *Visual Computing for Medicine (Second Edition)*, second edition ed. Morgan Kaufmann, Boston, 2014, pp. 229 – 267. 4

[PRH10] PRASSNI J.-S., ROPINSKI T., HINRICHS K.: Uncertainty-aware guided volume segmentation. *Visualization and Computer Graphics, IEEE Transactions on 16*, 6 (2010), 1358–1365. 11, 12, 17

[PRJ12] POTTER K., ROSEN P., JOHNSON C. R.: From quantification to visualization: A taxonomy of uncertainty visualization approaches. In *Uncertainty Quantification in Scientific Computing* (Berlin, Heidelberg, 2012), Springer Berlin Heidelberg, pp. 226–249. 2, 5

[PWH11] PÖTHKOW K., WEBER B., HEGE H.-C.: Probabilistic marching cubes. In *Computer Graphics Forum* (2011), vol. 30, Wiley Online Library, pp. 931–940. 12, 17

[PXP00] PHAM D. L., XU C., PRINCE J. L.: Current methods in medical image segmentation. *Annual Review of Biomedical Engineering 2*, 1 (2000), 315–337. 4

[RFCL16] RODRÍGUEZ J. H., FRAILE F. J. C., CONDE M. J. R., LLORENTE P. L. G.: Computer aided detection and diagnosis in medical imaging: A review of clinical and educational applications. In *Proceedings of the Fourth International Conference on Technological Ecosystems for Enhancing Multiculturality* (New York, NY, USA, 2016), TEEM '16, Association for Computing Machinery, p. 517–524. 4

[RGH*19] RISTOVSKI G., GARBERS N., HAHN H. K., PREUSSER T., LINSEN L.: Uncertainty-aware visual analysis of radiofrequency ablation simulations. *Computers & Graphics 79* (2019), 24 – 35. 15, 18

[RHH*20] REINHOLD J. C., HE Y., HAN S., CHEN Y., GAO D., LEE J.-H., PRINCE J. L., CARASS A.: Validating uncertainty in medical image translation. *2020 IEEE 17th International Symposium on Biomedical Imaging (ISBI)* (2020), 95–98. 8, 17

[RLBS03] RHODES P. J., LARAMEE R. S., BERGERON R. D., SPARR T. M.: Uncertainty visualization methods in isosurface volume rendering. In *Eurographics 2003, Short Papers* (2003), pp. 83–88. 14, 18

[RMW*17] RISTOVSKI G., MATUTE J., WEHRUM T., HARLOFF A., HAHN H. K., LINSEN L.: Uncertainty visualization for interactive assessment of stenotic regions in vascular structures. *Computers & Graphics 69* (2017), 116 – 130. 15, 16, 18

[ROP11] ROPINSKI T., OELTZE S., PREIM B.: Survey of glyph-based visualization techniques for spatial multivariate medical data. *Comput. Graph. 35*, 2 (2011), 392–401. 14

[RPB15] RONNEBERGER O., P.FISCHER, BROX T.: U-net: Convolutional networks for biomedical image segmentation. In *Medical Image Computing and Computer-Assisted Intervention (MICCAI)* (2015), vol. 9351 of *LNCS*, Springer, pp. 234–241. 12

[RPHL14] RISTOVSKI G., PREUSSER T., HAHN H. K., LINSEN L.: Uncertainty in medical visualization: Towards a taxonomy. *Computers & Graphics 39* (2014), 60 – 73. 1, 2, 3, 6

[RPSW10] RISHOLM P., PIEPER S., SAMSET E., WELLS W. M.: Summarizing and visualizing uncertainty in non-rigid registration. In *Medical Image Computing and Computer-Assisted Intervention – MICCAI 2010* (Berlin, Heidelberg, 2010), Springer Berlin Heidelberg, pp. 554–561. 10, 11, 17

[SFJ*16] SCHLACHTER M., FECHTER T., JURISIC M., SCHIMEK-JASCH T., OEHLKE O., ADEBAHR S., BIRKFELLNER W., NESTLE U., BÜHLER K.: Visualization of deformable image registration quality using local image dissimilarity. *IEEE Transactions on Medical Imaging 35*, 10 (2016), 2319–2328. 11, 17

[SFP*00] SCHIEMANN T., FREUDENBERG J., PFLESSER B., POMMERT A., PRIESMEYER K., RIEMER M., SCHUBERT R., TIEDE U., HÖHNE K.: Exploring the visible human using the voxel-man framework. *Computerized Medical Imaging and Graphics 24*, 3 (2000), 127–132. 5

[SHM10] SAAD A., HAMARNEH G., MOELLER T.: Exploration and visualization of segmentation uncertainty using shape and appearance prior information. In *IEEE Visualization (IEEE Vis)* (2010), pp. 1366–1375. 11, 12, 17

[SLK00] SZCZEPANIAK P., LISBOA P., KACPRZYK J.: *Fuzzy Systems in Medicine*. Springer, 01 2000. 10

[SMC*06] SIMPSON A. L., MA B., CHEN E. C. S., ELLIS R. E., STEWART A. J.: Using registration uncertainty visualization in a user study of a simple surgical task. In *Medical Image Computing and Computer-Assisted Intervention – MICCAI 2006* (Berlin, Heidelberg, 2006), Springer Berlin Heidelberg, pp. 397–404. 16, 18

[SMH10] SAAD A., MÖLLER T., HAMARNEH G.: ProbExplorer: Uncertainty-guided Exploration and Editing of Probabilistic Medical Image Segmentation. *Computer Graphics Forum* (2010). 15

[Smi13] SMITH R. C.: *Uncertainty Quantification: Theory, Implementation, and Applications*. Society for Industrial and Applied Mathematics, USA, 2013. 6

[SMS*18] SAAR G., MILLO C., SZAJEK L., BACON J., HERSCOVITCH P., KORETSKY A.: Anatomy, functionality, and neuronal connectivity with manganese radiotracers for positron emission tomography. *Molecular Imaging and Biology 20* (02 2018). 4

[SMV*14] SIMPSON A. L., MA B., VASARHELYI E. M., BORSCHNECK D. P., ELLIS R. E., JAMES STEWART A.: Computation and visualization of uncertainty in surgical navigation. *The International Journal of Medical Robotics and Computer Assisted Surgery 10*, 3 (2014), 332–343. 16, 18

[SP19] SAMEI E., PECK D. J.: *Physics of Radiation and Matter*. John Wiley & Sons, Ltd, 2019, ch. 1, pp. 1–54. 1

[SRM*19] SCHLACHTER M., RAIDOU R., MUREN L., PREIM B., PUTORA P., BÜHLER K.: State-of-the-art report: Visual computing in radiation therapy planning. *Computer Graphics Forum 38*, 3 (2019), 753–779. 15

[SSHM07] SAAD A., SMITH B., HAMARNEH G., MÖLLER T.: Simultaneous segmentation, kinetic parameter estimation, and uncertainty visualization of dynamic pet images. In *International Conference on Medical Image Computing and Computer-Assisted Intervention* (10 2007), pp. 726–733. 9, 17, 18

[SSK*16] SACHA D., SENARATNE H., KWON B. C., ELLIS G., KEIM D. A.: The Role of Uncertainty, Awareness, and Trust in Visual Analytics. *IEEE Transactions on Visualization and Computer Graphics (Proceedings of the Visual Analytics Science and Technology) 22*, 01 (Jan. 2016), 240–249. 20

[SWGS11] SIMPSON I. J. A., WOOLRICH M., GROVES A. R., SCHNABEL J. A.: Longitudinal brain mri analysis with uncertain registration. In *Medical Image Computing and Computer-Assisted Intervention – MICCAI 2011* (Berlin, Heidelberg, 2011), Springer Berlin Heidelberg, pp. 647–654. 11

[TS16] TIAN X., SAMEI E.: Accurate assessment and prediction of noise in clinical ct images. *Medical Physics 43*, 1 (2016), 475–482. 8, 17

[TWSM15] TORSNEY-WEIR T., SEDLMAIR M., MÖLLER T.: Decision making in uncertainty visualization. In *VDMU Workshop on Visualization for Decision Making under Uncertainty 2015* (October 2015). 1

[UHP*20] UNGER J., HEBISCH C., PHIPPS J. E., AO L. LAGARTO J., KIM H., DARROW M. A., BOLD R. J., MARCU L.: Real-time diagnosis and visualization of tumor margins in excised breast specimens using fluorescence lifetime imaging and machine learning. *Biomed. Opt. Express 11*, 3 (Mar 2020), 1216–1230. 15

[VZKL06] VILANOVA A., ZHANG S., KINDLMANN G., LAIDLAW D.: *An Introduction to Visualization of Diffusion Tensor Imaging and Its Applications*. Springer Berlin Heidelberg, Berlin, Heidelberg, 2006, pp. 121–153. 19

[WCW*17] WIESER H.-P., CISTERNAS E., WAHL N., ULRICH S., STADLER A., MESCHER H., MÜLLER L.-R., KLINGE T., GABRYS H., BURIGO L., ET AL.: Development of the open-source dose calculation and optimization toolkit matrad. *Medical Physics 44*, 6 (2017), 2556–2568. 15, 16, 18

[WHLS19] WANG J., HAZARIKA S., LI C., SHEN H.: Visualization and visual analysis of ensemble data: A survey. *IEEE Transactions on Visualization and Computer Graphics 25* (2019), 2853–2872. 20

[WSSM19] WINDHAGER F., SALISU S., SCHREDER G., MAYR E.: Uncertainty of what and for whom -and does anyone care? propositions for cultural collection visualization. 19

[WTW*08] WHITCHER B., TUCH D. S., WISCO J. J., SORENSEN A. G., WANG L.: Using the wild bootstrap to quantify uncertainty in diffusion tensor imaging. *Human Brain Mapping 29*, 3 (2008), 346–362. 9, 17

[YCMA12] YONG C., CHEW K. M., MAHMOOD N. H., ARIFFIN I.: A survey of visualization tools in medical imaging. *Procedia - Social and Behavioral Sciences 56* (10 2012), 265–271. 2

[YHS94] YI S., HARALICK R. M., SHAPIRO L. G.: Error propagation in machine vision. *Machine Vision and Applications 7*, 2 (Jun 1994), 93–114. 10

[YN15] YANG X., NIETHAMMER M.: Uncertainty quantification for lddmm using a low-rank hessian approximation. In *Medical Image Computing and Computer-Assisted Intervention – MICCAI 2015* (Cham, 2015), Springer International Publishing, pp. 289–296. 11, 17

[ZBDH*15] ZU BERGE C. S., DECLARA D., HENNERSPERGER C., BAUST M., NAVAB N.: Real-time uncertainty visualization for b-mode ultrasound. In *2015 IEEE Scientific Visualization Conference (SciVis)* (2015), IEEE, pp. 33–40. 8, 17

[ZSL*16] ZHANG C., SCHULTZ T., LAWONN K., EISEMANN E., VILANOVA A.: Glyph-based comparative visualization for diffusion tensor fields. *IEEE Trans. on Visualization and Computer Graphics 22*, 1 (2016), 797–806. 15, 18

[ZT03] ZHOU J., TÖNNIES K.: State of the art for volume rendering. *Technical Report* (08 2003). 14

https://www.overleaf.com/project/607562f7dc9a8a59bb17877d